

# ORGANOMETALLIC-MEDIATED RADICAL (CO)POLYMERIZATION OF $\gamma$ -METHYLENE- $\gamma$ -BUTYROLACTONE: ACCESS TO PH-RESPONSIVE POLY(VINYL ALCOHOL) DERIVATIVES

Zhuoqun Wang,<sup>†</sup> Rinaldo Poli,<sup>‡,§</sup> Christophe Detrembleur,<sup>†</sup> and Antoine Debuigne<sup>\*,†</sup>

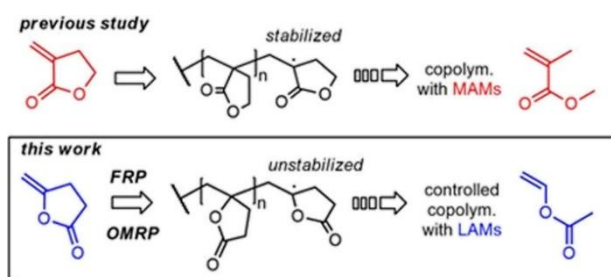
<sup>†</sup>Center for Education and Research on Macromolecules (CERM), CESAM Research Unit, Department of Chemistry, University of Liege, Allée de la Chimie B6A, 4000 Liège, Belgium

<sup>‡</sup>CNRS, LCC (Laboratoire de Chimie de Coordination) and Université de Toulouse, UPS, INPT, 205 route de Narbonne, BP 44099, 31077 Toulouse Cedex 4, France

<sup>§</sup>Institut Universitaire de France, 1, rue Descartes, 75231 Paris Cedex 05, France

## ABSTRACT

Conjugated vinyl lactones commonly serve as precursors of polymers with pendant cyclic esters, which can undergo several chemical modifications. They have notably been copolymerized with “more activated monomers” like (meth)acrylates. By contrast, the radical polymerization of nonconjugated methylene lactone analogues has been disregarded as well as their copolymerization with “less-activated monomers” such as acyclic vinyl esters. The present work explores the conventional radical polymerization and the reversible deactivation radical polymerization of  $\gamma$ -methylene- $\gamma$ -butyrolactone ( $\gamma$ M $\gamma$ BL) and its copolymerization with vinyl acetate (VAc). Statistical P( $\gamma$ M $\gamma$ BL-co-VAc) copolymers with predictable molar mass, low dispersity, and precise compositions were notably achieved by organometallic-mediated radical polymerization based on cobalt complexes via both reversible termination, also referred to as reversible chain deactivation, and degenerative chain-transfer pathways. Upon hydrolysis, these  $\gamma$ M $\gamma$ BL-containing (co)polymers release one alcohol moiety and one carboxylic group per repeating unit, leading to unprecedented carboxylic acid-functionalized poly(vinyl alcohol) derivatives. A preliminary study emphasizes the pH responsiveness of the latter in water.



## INTRODUCTION

Vinylidene lactones have received great interest in the last decade as building blocks for the production of bio-based specialty polymers.<sup>1</sup> Among them,  $\alpha$ -methylene- $\gamma$ -butyrolactone ( $\alpha$ M $\gamma$ BL),<sup>1</sup> or tulipalin A, can be isolated from tulips, whereas  $\beta$ -methyl- $\alpha$ -methylene- $\gamma$ -butyrolactone ( $\beta$ M $\alpha$ M $\gamma$ BL)<sup>2</sup> and  $\gamma$ -methyl- $\alpha$ -methylene- $\gamma$ -butyrolactone ( $\gamma$ M $\alpha$ M $\gamma$ BL)<sup>3</sup> are prepared from biomass-derived itaconic acid and levulinic acid, respectively (Scheme 1). Several approaches have been considered for the conversion of these methylene lactones into (co)polymers including ring-opening polymerization<sup>4-6</sup> leading to polyesters and also group transfer,<sup>7,8</sup> anionic,<sup>9</sup> zwitterionic,<sup>10-14</sup> coordination,<sup>15-18</sup> and radical<sup>19-25</sup> polymerizations providing polymers with a pendant five-membered ring.

The largely investigated radical polymerization of methylene lactones occurs via repeated radical addition onto their exocyclic double bond (Scheme 1). In this respect,  $\alpha$ M $\gamma$ BL derivatives can be considered as cyclic analogues of the petroleum-based methyl methacrylate (MMA). As a matter of fact, it belongs to the class of more activated monomers, which consist in conjugated monomers bearing a radical stabilizing group onto the double bond. Homopolymers with pendant butyrolactone moieties were notably prepared via conventional radical polymerization of  $\alpha$ M $\gamma$ BL<sup>19,20</sup> and  $\beta$ M $\alpha$ M $\gamma$ BL.<sup>21</sup> Compared to poly(MMA) (PMMA), these poly( $\alpha$ M $\gamma$ BL)s exhibit higher T<sub>g</sub> as well as increased optical properties.<sup>19,26</sup>

The conventional radical copolymerization of  $\alpha$ M $\gamma$ BL<sup>22,23,27-29</sup> or  $\gamma$ M $\alpha$ M $\gamma$ BL<sup>24,25</sup> with various conjugated vinyl monomers like MMA,<sup>22-24</sup> styrene,<sup>22,24,28</sup> acrylamide,<sup>27</sup> butyl acrylate,<sup>24</sup> exomethylene lactide,<sup>25</sup> and methacrylated oleic acid<sup>29</sup> is also reported. Interestingly, these  $\alpha$ -methylene lactones exhibit greater reactivity compared to their acyclic MMA counterpart because of the higher degree of delocalization of their radical species onto the carbonyl group of the rigid lactone.<sup>21</sup>

The synthesis of well-defined  $\alpha$ -methylene lactone-based (co)polymers was also achieved via reversible deactivation radical polymerization (RDRP). For example,  $\alpha$ M $\gamma$ BL-containing homopolymers<sup>30</sup> and block copolymers<sup>30-33</sup> with predictable molar masses and low dispersities were prepared via copper-catalyzed atom transfer radical polymerization (ATRP). High-density poly( $\alpha$ M $\gamma$ BL) brushes were also produced by surface-initiated ATRP of  $\alpha$ M $\gamma$ BL.<sup>34</sup> On the other hand,  $\alpha$ M $\gamma$ BL as well as its  $\gamma$ -substituted derivatives were polymerized in a controlled manner via reversible addition fragmentation chain transfer (RAFT).<sup>35</sup> The RAFT polymerization of  $\gamma$ M $\alpha$ M $\gamma$ BL and copolymerization with styrene were also performed under miniemulsion<sup>36</sup> and from ab initio emulsion<sup>37</sup> conditions.

Considering the higher reactivity of  $\alpha$ M $\gamma$ BL-based monomers compared to MMA,<sup>21</sup> their copolymerization with unconjugated less activated monomers (LAMs) including vinyl acetate (VAc) or  $\alpha$ -olefins is clearly jeopardized. However,  $\gamma$ -methylene- $\gamma$ -butyrolactone ( $\gamma$ M $\gamma$ BL), a cyclic structural analogue of VAc, appears as an ideal candidate for incorporating pendant lactones within LAM-based copolymers (Scheme 1). Surprisingly,  $\gamma$ M $\gamma$ BL has almost been completely disregarded in the polymerization field. To our knowledge, only one example relative to the tentative conventional radical copolymerization of  $\gamma$ M $\gamma$ BL and MMA is succinctly mentioned in the literature<sup>23</sup> and the reversible deactivation radical (co)polymerization of  $\gamma$ M $\gamma$ BL has never been reported. In the present work, we explored for the first time the conventional radical homopolymerization of  $\gamma$ M $\gamma$ BL as well as its copolymerization with VAc. Reactivity ratios were determined to gain insight into the distribution of the cyclic and acyclic ester moieties along the backbone. The reversible deactivation radical copolymerization of  $\gamma$ M $\gamma$ BL with VAc was also investigated through organometallic-mediated radical

polymerization (OMRP),<sup>38-41</sup> an efficient RDRP technique for controlling the polymerization of several LAMs including vinyl esters,<sup>42-44</sup> vinyl amides,<sup>45-48</sup> vinyl carbonates,<sup>49,50</sup> vinyl chloride,<sup>51</sup> vinylidene fluoride,<sup>52</sup> or ethylene.<sup>53-55</sup> Copolymerization conditions were optimized to produce poly( $\gamma$ M $\gamma$ BL-co-VAc) with predictable molar mass, low dispersity, and precise composition. Finally, few postpolymerization modifications of these poly( $\gamma$ M $\gamma$ BL-co-VAc) were carried out to produce unprecedented carboxylic acid-functionalized poly(vinyl alcohol)s (PVA) via hydrolysis of the pendant acyclic and cyclic esters. A preliminary study of the solution properties of these potentially pH-responsive polymers was also performed.

## EXPERIMENTAL SECTION

### Materials.

Cobalt(II) acetylacetonate (Co(acac)<sub>2</sub>) (97 %, Acros), 4-pentynoic acid (98 %, Fluorochem), 2,2,6,6-tetramethylpiperidine 1-oxyl (TEMPO) (98 %, Aldrich), 2,2'-azobis(4-methoxy-2,4-dimethyl valeronitrile) (V-70,  $t^{1/2}$  = 10 h at 30 °C) (>98 %, Wako), and 2,2'-azobisisobutyronitrile (AIBN,  $t^{1/2}$  = 10 h at 65 °C) (98 %, Aldrich) were used as received. Sodium hydroxide (NaOH,  $\geq$ 97 %, Acros), silica gel for column chromatography (60 Å, ROCC S.A.), tetrahydrofuran (THF,  $\geq$ 99.9 %, VWR), chloroform (>99 %, VWR), methanol (MeOH,  $\geq$ 99.8 %, VWR), *n*-heptane (>99.6 %, VWR), *n*-hexane (>99 %, VWR), ethyl acetate ( $\geq$ 99.9 %, VWR), and acetonitrile ( $\geq$ 99.99 %, Acros) were used as received. *N,N*-Dimethylformamide (DMF, >99 %, VWR) was dried over molecular sieves prior to use. Dichloromethane (CH<sub>2</sub>Cl<sub>2</sub>) was degassed and dried over 4 Å molecular sieves. VAc (>99 %, Aldrich) was dried under calcium hydride, purified by distillation under reduced pressure, and degassed by freeze-drying cycle under vacuum. The alkyl-cobalt(III) adduct initiator (PVAc<sub>c<4</sub>-Co(acac)<sub>2</sub>), [Co(acac)<sub>2</sub>-(CH(OAc)-CH<sub>2</sub>)<sub>c<4</sub>R<sub>0</sub>], R<sub>0</sub> being the primary radical generated by 2,2'-azo-bis(4-methoxy-2,4-dimethyl valeronitrile) (V-70, Wako), was prepared as described previously<sup>43</sup> and stored as a CH<sub>2</sub>Cl<sub>2</sub> solution at -20 °C under argon. Dialyses were carried out with a Spectra/Por dialysis membrane (pretreated RC tubing 1 kDa).

### Characterization.

Size exclusion chromatography (SEC) of poly( $\gamma$ -methylene- $\gamma$ -butyrolactone) (P $\gamma$ M $\gamma$ BL) and of P( $\gamma$ M $\gamma$ BL-co-VAc) with  $F_{\gamma\text{M}\gamma\text{BL}} > 0.5$  was carried out in DMF containing 0.025 M of LiBr at 55 °C with a Waters chromatograph equipped with three columns (Waters Styragel PSS GRAM 1000 Å (x2), 30 Å), a dual  $\lambda$  absorbance detector (Waters 2487), and a refractive index detector (Waters 2414). The system was operated at a flow rate of 1 mL/min. A polystyrene calibration was used. SEC analyses of P( $\gamma$ M $\gamma$ BL-co-VAc) with  $F_{\gamma\text{M}\gamma\text{BL}} < 0.5$  were carried out in THF at 45 °C at a flow rate of 1 mL/min with a Viscotek 305 TDA liquid chromatograph equipped with 2 PSS SDV linear M columns calibrated with PS. <sup>1</sup>H nuclear magnetic resonance (NMR), heteronuclear single quantum coherence (HSQC), and correlation spectroscopy (COSY) spectra were recorded at 298 K with a Bruker AVANCE III HD spectrometer ( $B_0$  = 9.04 T) (400MHz) and treated with MestreNova software. Infrared (IR) spectra were recorded on a Thermo Fisher Scientific Nicolet IS5 equipped with an ATR ID5 module using a diamond crystal (650–4000cm<sup>-1</sup>). Differential scanning calorimetry (DSC) was performed on a TA Instruments Q1000 differential scanning calorimeter, using hermetic aluminum pans, an indium standard for calibration, nitrogen as the purge gas, and a sample weight of about 5 mg. The sample was cooled down to -40 °C at a cooling rate of 40 °C/min, followed by an isotherm at -40 °C for 2min and heating up to 120 °C at

10 °C/min heating rate. This cycle was repeated twice. Thermogravimetric analysis (TGA) was carried out with a Hi-Res TGA Q500 from TA Instruments under nitrogen at a heating rate of 20 °C/min from ambient temperature to 600 °C at a heating rate of 20 °C/min.

### Computational Details.

The computational work was carried out using the Gaussian09 suite of programs.<sup>56</sup> Gas-phase geometry optimizations were performed without any symmetry constraint using the BPW91\* functional, which is a reparameterized version of B3PW91 with the same parameters previously optimized for B3LYP,<sup>57</sup> and the 6-311G(d,p) basis functions for all light atoms (H, C, O, Si), whereas the Co atom was treated with the SDD basis set augmented by an f polarization function ( $\alpha = 2.780$ ).<sup>58</sup> A correction for dispersion was also included during the geometry optimizations using Grimme's D3 empirical method (BPW91\*-D3), using SR6 and S8 parameters identical to those optimized for B3PW91.<sup>59</sup> The unrestricted formulation was used for open-shell molecules, yielding only minor spin contamination ( $\langle S^2 \rangle$ ) at convergence was very close to the expected values of 0.75 for doublet states and 3.75 for the quartet state). All final geometries were characterized as local minima by verifying that all second derivatives of the energy were positive. Thermochemical corrections were obtained at 298.15 K on the basis of frequency calculations, using the standard approximations (ideal gas, rigid rotor, and harmonic oscillator). A further correction of 1.95 kcal/mol was applied to bring the *G* values from the gas phase (1 atm) to the solution (1 mol/L) standard state.<sup>60</sup> The Cartesian coordinates and energies of all optimized structures are available in the Supporting Information (Table S5).

### Synthesis of $\gamma$ -Methylene- $\gamma$ -butyrolactone ( $\gamma$ M $\gamma$ BL).

4-Pentynoic acid (2.00 g, 20.4 mmol) and Pd(OAc)<sub>2</sub> (0.023 g, 0.10 mmol) were placed under argon in a 100 mL flask and dissolved in degassed CHCl<sub>3</sub> (30 mL). The reaction mixture was then heated at 50 °C under stirring for 24 h. After cooling the reaction mixture to room temperature, CHCl<sub>3</sub> was evaporated under reduced pressure. The reaction mixture was purified by column chromatography (hexane/ethyl acetate: 7/3 (v/v), *R<sub>f</sub>* of  $\gamma$ M $\gamma$ BL = 0.58). Accordingly,  $\gamma$ M $\gamma$ BL was collected as a colorless liquid (1.47 g) in a 73 % yield. <sup>1</sup>H NMR (400 MHz, CDCl<sub>3</sub>):  $\delta$  4.74 (d, *J* = 2.3 Hz, 1H), 4.32 (d, *J* = 2.0 Hz, 1H), 2.94–2.85 (m, 2H), 2.73–2.58 (m, 2H). <sup>13</sup>C NMR (101 MHz, CDCl<sub>3</sub>):  $\delta$  174.92, 155.70, 88.64, 29.84, 25.06. IR (cm<sup>-1</sup>) 2927, 1802, 1668, 1445, 1292, 1119, 1005, 968, 881, 838, 662.

### Conventional Radical Polymerization of $\gamma$ M $\gamma$ BL.

AIBN (0.082 g, 0.50 mmol) and  $\gamma$ M $\gamma$ BL (0.98 g, 10 mmol) were placed in a 15 mL Schlenk tube, degassed by three freeze–pump–thaw cycles and placed under argon and then heated at 70 °C. After 24 h. the samples were withdrawn for determining the molecular parameters (*M<sub>n</sub>*, *D*) by SEC in DMF using a PS calibration. The conversion was determined by gravimetry. The homopolymer was dissolved in acetonitrile and purified via repeated precipitations (three times) in methanol and dried under vacuum overnight at 80 °C before characterization by <sup>1</sup>H NMR, <sup>13</sup>C NMR, HSQC, and COSY in CD<sub>3</sub>CN.

### Conventional Radical Copolymerization of $\gamma$ M $\gamma$ BL and VAc.

V-70 (0.31 g, 1.0 mmol) and  $\gamma$ M $\gamma$ BL (0.78 g, 8.0 mmol) were placed in a 15 mL Schlenk tube, degassed by three freeze–pump–thaw cycles and placed under argon. After the addition of degassed VAc (1.10 mL, 1.03 g, 12.0 mmol), the polymerization medium (*f*<sup>o</sup> <sub>$\gamma$ M $\gamma$ BL</sub> = 0.4) was heated at 40 °C. After 24 h. the samples were withdrawn for determining the conversion by <sup>1</sup>H NMR in CDCl<sub>3</sub> and the molecular parameters (*M<sub>n</sub>*, *D*) by SEC in THF. The final copolymer was purified via repeated precipitations (three

times) in *n*-heptane and dried under vacuum overnight at 80 °C before characterization by <sup>1</sup>H NMR, <sup>13</sup>C NMR, HSQC, and COSY in CDCl<sub>3</sub>.

A similar experiment was carried out with a different initial comonomer feed ratio, namely  $f^{\circ}_{\gamma\text{M}\gamma\text{BL}} = 0.2$ , keeping constant all other parameters (40 °C, [comonomers]<sub>0</sub>/[V-70]<sub>0</sub> = 100/5).

### Determination of Reactivity Ratios for Radical Copolymerization of $\gamma\text{M}\gamma\text{BL}$ and VAc.

A series of  $\gamma\text{M}\gamma\text{BL}$ /VAc copolymerizations were carried out in bulk at 40 °C with different comonomer ratios ( $0.1 < f^{\circ}_{\gamma\text{M}\gamma\text{BL}} < 0.7$ ) using V-70 as the initiator ([comonomers]<sub>0</sub>/[V-70]<sub>0</sub> = 100/3). Copolymerizations were stopped at low conversion to avoid significant composition drift. Conversions were determined by <sup>1</sup>H NMR in CDCl<sub>3</sub>. The copolymers were purified by repeated precipitation in heptane (three times) and dried at 50 °C under reduced pressure. The molar fractions of the comonomers in the copolymer ( $F_{\gamma\text{M}\gamma\text{BL}}$  and  $F_{\text{VAc}}$ ) were determined by <sup>1</sup>H NMR in CDCl<sub>3</sub>. These data, provided in Table S1, were then used for the determination of the reactivity ratios via three methods described below.

- (i) The Fineman–Ross (FR) linearization method<sup>61</sup> which generates a straight line whose slope and intercept with the ordinate (Y-axis) correspond, respectively, to  $r_1$  and  $r_2$  (eq 1).

$$f(F - 1) / F = r_1(f^2 / F) - r_2 \quad (1)$$

where  $f = f_1 / f_2$  and  $F = F_1 / F_2$ .

- (ii) The Kelen–Tüdös (KT) method<sup>62</sup> which involves parameters  $\eta$  and  $\zeta$ , the mathematical functions of the mole ratios in the monomer feed ( $f$ ) and in the copolymer ( $F$ ) and of a parameter  $\alpha$  calculated on the basis of the lowest and highest values of  $(f^2 / F)$ . The determination of  $r_1$  and  $r_2$  is made possible by the extrapolation and the interception at  $\xi = 1$  and  $\xi = 0$ , giving respectively  $r_1$  and  $(-r_2 / \alpha)$  (eq 2).

$$\eta = (r_1 + (r_2 / \alpha))\zeta - (r_2 / \alpha) \quad (2)$$

where  $\eta = (f(F - 1)) / (F(\alpha + (f^2 / F)))$ ;  $\zeta = (f^2 / F) / (\alpha + (f^2 / F))$ ;  $\alpha = ((f^2 / F)_{\text{max}} \times (f^2 / F)_{\text{min}})^{0.5}$ .

- (iii) The nonlinear least-squares method<sup>63,64</sup> based on the Mayo–Lewis equation (eq 3).

$$F_1 = (r_1 f_1^2 + f_1 f_2) / (r_1 f_1^2 + 2f_1 f_2 + r_2 f_2^2) \quad (3)$$

Based on the reactivity ratio, the Skeist model<sup>65</sup> (eqs 4 and 5) was used to predict the cumulative and instantaneous copolymer composition ( $F_{\text{cumul}}$  and  $F_{\text{inst}}$ ) as a function of the monomer conversion.

$$\begin{aligned} \text{Conv} &= 1 - (M / M_0) \\ &= 1 - [(f_1 / f_1^{\circ})^{\alpha} (f_2 / f_2^{\circ})^{\beta} [(f_1^{\circ} - \delta) / (f_1 - \delta)]^{\gamma}] \end{aligned} \quad (4)$$

where  $M_0$  and  $M$  are the initial and the instantaneous monomer concentration,  $f^{\circ}$  and  $f$  correspond to the initial and the instantaneous mole fraction in the feed, and  $\alpha$ ,  $\beta$ ,  $\delta$ , and  $\gamma$  are defined as follows:  $\alpha = r_2 / (1 - r_2)$ ;  $\beta = r_1 / (1 - r_1)$ ;  $\gamma = (1 - r_1 r_2) / ((1 - r_1)(1 - r_2))$ ;  $\delta = (1 - r_2) / (2 - r_1 - r_2)$ .

$$F_{1 \text{ cumul}} = [f_1^{\circ} - f_1(1 - \text{conv})] / \text{conv} \quad (5)$$

### OMRP of $\gamma\text{M}\gamma\text{BL}$ via Reversible Termination.

$\gamma\text{M}\gamma\text{BL}$  (0.98 g, 10 mmol) was placed in a 15 mL Schlenk tube, degassed by three freeze–pump–thaw cycles and placed under argon. A solution of alkyl-cobalt(III) initiator (PVAc-<sub>4</sub>-Co(acac)<sub>2</sub>) in CH<sub>2</sub>Cl<sub>2</sub> (0.18 mL of a 0.111 M stock solution, 0.020 mmol) was added to  $\gamma\text{M}\gamma\text{BL}$  followed by the evaporation of

CH<sub>2</sub>Cl<sub>2</sub> under reduced pressure at room temperature. The reaction mixture ([ $\gamma$ M $\gamma$ BL]<sub>0</sub>/[PVAc<sub><4-</sub>Co(acac)<sub>2</sub>]<sub>0</sub> = 500/1) was heated at 40 °C for 24 h. After 24 h. one sample was taken and added with TEMPO (1 mg/0.1 mL of sample) to quench the polymerization before determining the conversion by gravimetry. Another sample was taken and dissolved in DMF (containing 10 mg of TEMPO per mL of DMF) before determining the molecular parameters ( $M_n$ ,  $\bar{D}$ ) by SEC calibrated with polystyrene in DMF. Finally, the polymerization mixture was quenched by the addition of TEMPO (0.20 g) dissolved in DMF (1 mL). The final copolymer was purified by precipitation in methanol (three times) and dried overnight under vacuum at 80 °C before characterization via <sup>1</sup>H NMR, <sup>13</sup>C NMR, HSQC, and COSY in CD<sub>3</sub>CN.

#### **Organometallic-Mediated Radical Copolymerization of $\gamma$ M $\gamma$ BL and VAc via Reversible Termination.**

$\gamma$ M $\gamma$ BL (0.49 g, 5.0 mmol) was placed in a 15 mL Schlenk tube, degassed by three freeze–pump–thaw cycles and placed under argon. A solution of alkyl-cobalt(III) initiator (PVAc<sub><4-</sub>Co(acac)<sub>2</sub>) in CH<sub>2</sub>Cl<sub>2</sub> (0.78 mL of a 0.064 M stock solution, 0.05 mmol) was added to  $\gamma$ M $\gamma$ BL followed by the evaporation of CH<sub>2</sub>Cl<sub>2</sub> under reduced pressure at room temperature. Finally, degassed VAc (1.84 mL, 1.72 g, 20 mmol) was injected under argon. The reaction mixture ( $f^{\circ}_{\gamma\text{M}\gamma\text{BL}} = 0.2$  and  $f^{\circ}_{\text{VAc}} = 0.8$ , [VAc]<sub>0</sub>/[ $\gamma$ M $\gamma$ BL]<sub>0</sub>/[PVAc<sub><4-</sub>Co(acac)<sub>2</sub>]<sub>0</sub> = 400/100/1) was heated at 40 °C for 12 h. The samples were regularly taken and added with TEMPO to quench the polymerization. The monomer conversion was determined by <sup>1</sup>H NMR in CDCl<sub>3</sub> (1 mg of TEMPO was added per milliliter of CDCl<sub>3</sub>). The molecular parameters ( $M_n$ ,  $\bar{D}$ ) of the polymer were determined by SEC in THF using a polystyrene calibration (the samples were dissolved in THF containing 10 mg of TEMPO/mL of THF). After 12 h. the polymerization mixture was quenched by the addition of TEMPO (0.20 g) dissolved in DMF (1 mL). The final copolymer was purified by precipitation in *n*-heptane (three times) and dried overnight under vacuum at 80 °C before characterization via <sup>1</sup>H NMR, <sup>13</sup>C NMR, HSQC, and COSY in CDCl<sub>3</sub>.

Similar experiments were carried out with different monomer initiator ratios, keeping constant all other parameters ( $f^{\circ}_{\gamma\text{M}\gamma\text{BL}} = 0.2$ , 40 °C, bulk): [VAc]<sub>0</sub>/[ $\gamma$ M $\gamma$ BL]<sub>0</sub>/[PVAc<sub><4-</sub>Co(acac)<sub>2</sub>]<sub>0</sub> = 800/200/1 and 200/50/1. The initial comonomer feed ratio was also varied ( $f^{\circ}_{\gamma\text{M}\gamma\text{BL}} = 0.4$  and 0.7), keeping constant all other parameters (40 °C, bulk, [comonomers]<sub>0</sub>/[PVAc<sub><4-</sub>Co(acac)<sub>2</sub>]<sub>0</sub> = 500). Note that the copolymer produced from  $f^{\circ}_{\gamma\text{M}\gamma\text{BL}} = 0.7$  was recovered by precipitation in methanol instead of heptane.

#### **OMRP of $\gamma$ M $\gamma$ BL via Degenerative Chain Transfer.**

$\gamma$ M $\gamma$ BL (0.98 g, 10 mmol) was placed in a 15 mL Schlenk tube. After degassing by three freeze–pump–thaw cycles, the degassed  $\gamma$ M $\gamma$ BL was transferred to a 15 mL Schlenk tube with Co(acac)<sub>2</sub> (0.005 g, 0.02 mmol) and AIBN (0.0099 g, 0.06 mmol) under argon. The reaction mixture ([ $\gamma$ M $\gamma$ BL]<sub>0</sub>/[AIBN]<sub>0</sub>/[Co(acac)<sub>2</sub>]<sub>0</sub> = 500/3/1) was heated at 70 °C for 24 h. and the samples were regularly taken from the reaction mixture and added with TEMPO to quench the polymerization. The monomer conversion was determined by gravimetry after the addition of TEMPO (1 mg/0.1 mL of sample). The molecular parameters ( $M_n$ ,  $\bar{D}$ ) of the polymer were determined by SEC in DMF using a polystyrene calibration (the samples were dissolved in DMF containing 10 mg of TEMPO/mL of DMF). After 24 h. the polymerization mixture was quenched by the addition of TEMPO (0.20 g) dissolved in DMF (1 mL). The final copolymer was purified by precipitation in methanol (three times) and dried overnight under vacuum at 80 °C before characterization via <sup>1</sup>H NMR, <sup>13</sup>C NMR, HSQC, and COSY in CD<sub>3</sub>CN.

A similar experiment was conducted at 40 °C using V-70 instead of AIBN ([ $\gamma$ M $\gamma$ BL]<sub>0</sub>/[V-70]<sub>0</sub>/[Co(acac)<sub>2</sub>]<sub>0</sub> = 500/3/1).

### Organometallic-Mediated Radical Copolymerization of $\gamma$ M $\gamma$ BL and VAc via Degenerative Chain Transfer.

$\gamma$ M $\gamma$ BL (0.49 g, 5.0 mmol) was degassed by three freeze–pump–thaw cycles and transferred to a 15 mL Schlenk tube with Co(acac)<sub>2</sub> (0.013 g, 0.05 mmol) and V-70 (0.046 g, 0.15 mmol) under argon. Degassed VAc (1.84 mL, 1.72 g, 20 mmol) was injected under argon. The reaction mixture ( $f^\circ_{\gamma\text{M}\gamma\text{BL}} = 0.2$ ,  $[\text{VAc}]_0/[\gamma\text{M}\gamma\text{BL}]_0/[\text{V-70}]_0/[\text{Co}(\text{acac})_2]_0 = 400/100/3/1$ ) was heated at 40 °C for 28 h. The samples were regularly picked out of the tube and added with traces of TEMPO to quench the polymerization. The monomer conversion and the molecular parameters ( $M_n$ ,  $\bar{D}$ ) of the polymer were determined by <sup>1</sup>H NMR in CDCl<sub>3</sub> and SEC calibrated with polystyrene in THF, respectively. After 28 h. the polymerization mixture was quenched by the addition of 1 mL of TEMPO in THF (0.20 g/mL). The final copolymer was purified by precipitation in heptane (three times) and dried overnight under vacuum at 80 °C before characterization via <sup>1</sup>H NMR, <sup>13</sup>C NMR, HSQC, and COSY in CDCl<sub>3</sub>.

### Synthesis of PVAc-b-P( $\gamma$ M $\gamma$ BL-co-VAc) Block Copolymer by OMRP.

A solution of alkyl-cobalt(III) initiator (PVAc<sub><4</sub>-Co(acac)<sub>2</sub>) in CH<sub>2</sub>Cl<sub>2</sub> (0.23 mL of a 0.111 M stock solution, 0.025 mmol) was added into a 15 mL Schlenk tube followed by the evaporation of CH<sub>2</sub>Cl<sub>2</sub> under reduced pressure at room temperature. Degassed VAc (1.20 mL, 1.08 g, 12.5 mmol) was injected under argon at 40 °C. After 3 h. a sample was picked out of the tube and added with traces of TEMPO (~10 mg/mL) to quench the polymerization for determining the monomer conversion by <sup>1</sup>H NMR in CDCl<sub>3</sub> (conversion = 27 %) and the molecular parameters of the PVAc precursor (10 000 g/mol,  $\bar{D} = 1.06$ ) by SEC<sub>THF cal PS</sub>. Then, unreacted VAc was evaporated under reduced pressure at room temperature. The degassed mixture of  $\gamma$ M $\gamma$ BL (0.25 g, 2.5 mmol) and VAc (0.96 mL, 0.86 g, 10 mmol) was injected under argon. The polymerization medium was heated at 40 °C for 15 h. and the samples were regularly taken and added with traces of TEMPO to quench the polymerization. The monomer conversion and the molecular parameters ( $M_n$ ,  $\bar{D}$ ) of the polymer were determined by <sup>1</sup>H NMR in CDCl<sub>3</sub> and SEC<sub>THF cal PS</sub>, respectively. After 15 h. the polymerization mixture was quenched by the addition of 1 mL of TEMPO in THF (0.20 g/mL) (global conv = 59 %,  $M_n$  SEC THF cal PS 19000 g/mol,  $\bar{D} = 1.43$ ). The final copolymer was purified by precipitation in *n*-heptane (three times) and dried overnight under vacuum at 80 °C before characterization via <sup>1</sup>H NMR, <sup>13</sup>C NMR, HSQC, and COSY in CDCl<sub>3</sub>.

### Base Hydrolysis of poly( $\gamma$ M $\gamma$ BL-co-VAc).

Poly( $\gamma$ M $\gamma$ BL-co-VAc) (1 g, 13 800 g/mol,  $F_{\gamma\text{M}\gamma\text{BL}} = 0.32$ ) was dissolved in THF (10 mL). NaOH (1 g, 25 mmol) in deionized water (10 mL) was added to the reaction mixture followed by stirring at room temperature for 48 h. The solution was then dialyzed (membrane 1 kDa) against distilled water for 48 h followed by lyophilization. The copolymer, recovered as a powder, was characterized via <sup>1</sup>H NMR, <sup>13</sup>C NMR, HSQC, and COSY in D<sub>2</sub>O and by Fourier transform infrared spectroscopy.

## RESULTS AND DISCUSSION

### Synthesis and Conventional Radical Polymerization of $\gamma$ M $\gamma$ BL.

A straightforward synthesis of methylene lactones consists in the cycloisomerization of  $\gamma$ -alkynoic acids catalyzed by palladium,<sup>66,67</sup> gold,<sup>68,69</sup> copper,<sup>70,71</sup> or cobalt<sup>72</sup> complexes. Inspired by a recent report,<sup>67</sup>

we prepared the five-membered ring  $\gamma$ M $\gamma$ BL through cycloisomerization of 4-pentyn-1-ol acid using 0.5 mol % of Pd(OAc)<sub>2</sub> as the catalyst (Scheme 2A).

Compared to the original work,<sup>67</sup> water was replaced by chloroform as solvent to avoid the hydrolysis of the targeted lactone into 4-oxo-pentynoic acid. The conversion of 4-pentyn-1-ol acid reached 77 % after 45 h at room temperature but was almost complete after 24 h when performed at 50 °C, as indicated by the <sup>1</sup>H NMR spectrum in Figure S1b. The vinyl lactone was then isolated in a 70 % yield by silica gel chromatography and stored under nitrogen at -6 °C before use in polymerization. <sup>1</sup>H and <sup>13</sup>C NMR spectra (Figure S1c and S1d, respectively) confirmed the structure and the purity of  $\gamma$ M $\gamma$ BL. Note that neither  $\gamma$ M $\gamma$ BL nor  $\gamma$ -alkynoic acid can be extracted from the biomass.

The conventional radical homopolymerization of  $\gamma$ M $\gamma$ BL was first tested in bulk using a low-temperature azo-initiator, namely 2,2'-azobis(4-methoxy-2,4-dimethyl valeronitrile) (V70), at 40 °C (Scheme 2b), but no polymerization occurred under these conditions (Table 1, entry 1). However, the conversion of  $\gamma$ M $\gamma$ BL reached 41 % when the polymerization was conducted at 70 °C using 5 mol % of azobis(isobutyronitrile) (AIBN) as the initiator (Table 1, entry 2). P $\gamma$ M $\gamma$ BL with  $M_{n, SEC}$  of 4200 g/mol and a dispersity of 1.89 was obtained. The <sup>1</sup>H NMR (Figure 1a) as well as the COSY and HSQC (Figure S2) experiments confirmed the structure of P $\gamma$ M $\gamma$ BL.

Next, we considered the conventional radical copolymerization of  $\gamma$ M $\gamma$ BL with its acyclic analogue, that is, VAc (Scheme 2c). The  $\gamma$ M $\gamma$ BL/VAc copolymerization was carried out in bulk for 24 h at 40 °C in the presence of 5 mol % of V70. Two initial molar fractions of  $\gamma$ M $\gamma$ BL ( $f_{\gamma M \gamma BL}^0$ ) were considered, that is, 0.2 and 0.4 (Table 1, entries 3 and 4). In both cases, the comonomer conversion exceeded 50 %. After isolation by precipitation in heptane, the polymers were analyzed not only by <sup>1</sup>H NMR (Figure 1b) but also by COSY and HSQC (Figure S3). The latter confirmed the presence of  $\gamma$ M $\gamma$ BL and VAc units in both products. The incorporation of  $\gamma$ M $\gamma$ BL within the copolymer was quantified by <sup>1</sup>H NMR by comparing the relative intensity of the signal corresponding to the methylene protons e of  $\gamma$ M $\gamma$ BL units at 2.6 ppm and the signal b assigned to the methine protons of VAc units around 5 ppm. Accordingly, we found that 19 and 32 mol % of  $\gamma$ M $\gamma$ BL were respectively incorporated in P( $\gamma$ M $\gamma$ BL-co-VAc)s (Table 1 entries 3 and 4, respectively). Interestingly, the molar fraction of  $\gamma$ M $\gamma$ BL in the copolymer ( $F_{\gamma M \gamma BL}$ ) was only slightly lower than its molar fraction in the initial feed ( $f_{\gamma M \gamma BL}^0$ ). This observation was further corroborated by the subsequently measured reactivity ratios.

To determine the  $\gamma$ M $\gamma$ BL/VAc reactivity ratios and get insight into the distribution of the  $\gamma$ M $\gamma$ BL and VAc units, a series of copolymerizations with different initial feed compositions ( $f_{\gamma M \gamma BL}^0$  ranging from 0.1 to 0.7) were initiated by V70 in bulk at 40 °C (Table S1). Polymerizations were stopped at a low conversion to prevent significant composition drift. The copolymers were purified by precipitation in heptane before measuring their composition by <sup>1</sup>H NMR as described above. These experimental data were then used to determine the reactivity ratios by FR<sup>61</sup> (Figure 2a) and KT<sup>61</sup> (Figure 2b) linearization methods and by the nonlinear least-squares fitting method based on the Mayo Lewis equation<sup>63,64</sup> (NL, Figure 2c). Note that the reactivity ratios obtained by these methods are highly consistent ( $r_{\gamma M \gamma BL} = 0.2$ ,  $r_{VAc} = 1.05$ ). The low value of  $r_{\gamma M \gamma BL}$  is in agreement with its low tendency to homopolymerize at 40 °C. On the other hand,  $r_{VAc}$  close to 1 indicates that radical chains with a VAc terminal unit react almost randomly with  $\gamma$ M $\gamma$ BL and VAc. Based on these reactivity ratio values, we also evaluated the possible composition drift along the P( $\gamma$ M $\gamma$ BL-co-VAc) copolymer using the Skeist model.<sup>65</sup> Figure 2d represents the evolution of the cumulative ( $F_{\gamma M \gamma BL, cumul}$ ) and instantaneous ( $F_{\gamma M \gamma BL, inst}$ ) molar fractions of  $\gamma$ M $\gamma$ BL in the P( $\gamma$ M $\gamma$ BL-co-VAc) copolymer as a function of the overall molar monomer conversion when using

40 mol % of  $\gamma\text{M}\gamma\text{BL}$  in the initial feed ( $f_{\gamma\text{M}\gamma\text{BL}}^{\circ} = 0.4$ ). As a confirmation of the validity of this model, the cumulative composition of the P( $\gamma\text{M}\gamma\text{BL-co-VAc}$ ) copolymer ( $F_{\gamma\text{M}\gamma\text{BL}} = 0.32$ ) formed at 54 % of overall conversion (Table 1, entry 4) is in agreement with the cumulative molar fraction of  $\gamma\text{M}\gamma\text{BL}$  predicted at this conversion by the Skeist model (see Figure 2d,  $F_{\gamma\text{M}\gamma\text{BL cumul}} = 0.33$ ). Interestingly, the instantaneous composition ( $F_{\gamma\text{M}\gamma\text{BL inst}}$ ) remains relatively constant at least until 60 % conversion and suggests a low drift of the composition along the polymerization. At higher conversion, the Skeist curve indicates a significant increase of the  $\gamma\text{M}\gamma\text{BL}$  content in the copolymer. Nevertheless, one must keep in mind that incorporating more than 50 % of this monomer within the copolymer is difficult given its low propensity to homopolymerize. The knowledge of the insertion mode of the comonomers within P( $\gamma\text{M}\gamma\text{BL-co-VAc}$ ) copolymers is a major asset for addressing their precision synthesis via reversible deactivation radical polymerization.

### Reversible Deactivation Radical (Co)polymerization of $\gamma\text{M}\gamma\text{BL}$ .

As a reminder, a high level of control was achieved for the OMRP of VAc, the acyclic analogue of  $\gamma\text{M}\gamma\text{BL}$ , when  $\text{Co}(\text{acac})_2$  was used as the controlling agent.<sup>43,44</sup> The equilibrium between the alkyl-cobalt(III) dormant species and the active radical species occurred via reversible cleavage of the Co–C bond at a moderate temperature. Typically, the polymerization of VAc proceeded in a controlled manner when carried out in bulk at 40 °C using a preformed  $\text{PVAc}_{\sim 4}\text{-Co}(\text{acac})_2$  species as the initiator (Scheme 3). Under these conditions, PVAc with low dispersity ( $\mathcal{D} \approx 1.1$ ) and predictable molar mass was formed.<sup>44</sup> Considering the structural similarities between VAc and  $\gamma\text{M}\gamma\text{BL}$ , the homopolymerization of vinyl lactone was tested first under the same conditions, namely 40 °C, in bulk, with  $\text{PVAc}_{\sim 4}\text{-Co}(\text{acac})_2$  species as the initiator [ $\gamma\text{M}\gamma\text{BL}$ ]/[ $\text{PVAc}_{\sim 4}\text{-Co}(\text{acac})_2$ ] = 500 (Table S2, entry 1). However, the polymerization stopped after 6 h (conversion = 9 %), and no evolution of the molar mass was observed along the polymerization ( $M_{n, \text{SEC}} \approx 7000$  g/mol,  $\mathcal{D} \approx 1.6\text{--}1.7$ ), suggesting an uncontrolled process. Note that very similar results were obtained when repeating the same experiment at 65 °C (Table S2, entry 2). Such a low tendency of  $\gamma\text{M}\gamma\text{BL}$  to propagate via OMRP most probably results from premature irreversible termination reactions.

To gain insight in the OMRP of  $\gamma\text{M}\gamma\text{BL}$  and to prepare novel polymer structures, we considered the reversible deactivation radical copolymerization of  $\gamma\text{M}\gamma\text{BL}$  and VAc (Scheme 3). A series of organometallic-mediated radical copolymerizations of  $\gamma\text{M}\gamma\text{BL}$  and VAc were first carried out in bulk at 40 °C with the  $\text{PVAc}_{\sim 4}\text{-Co}(\text{acac})_2$  initiator (Table 2). Three initial composition feeds were considered with the  $\gamma\text{M}\gamma\text{BL}$  molar fraction ( $f_{\gamma\text{M}\gamma\text{BL}}^{\circ}$ ) ranging from 0.2 to 0.7. The molecular parameters ( $M_n$  and  $\mathcal{D}$ ) of the copolymer and the monomer conversion were monitored throughout the polymerization via SEC and  $^1\text{H}$  NMR, respectively. At the desired time/conversion, TEMPO was added to the reaction medium to trap irreversibly the radical chains and stop the polymerization. The content of  $\gamma\text{M}\gamma\text{BL}$  in the final copolymer ( $F_{\gamma\text{M}\gamma\text{BL}}$ ), measured by  $^1\text{H}$  NMR, is indicated in Table 2. A representative spectrum is provided in Figure S4a. The structure of the P( $\gamma\text{M}\gamma\text{BL-co-VAc}$ ) copolymer is also confirmed by the COSY and HSQC spectra (Figure S4b,c).

Regardless of the initial composition feed,  $\text{PVAc}_{\sim 4}\text{-Co}(\text{acac})_2$  successfully initiated the  $\gamma\text{M}\gamma\text{BL/VAc}$  copolymerization at 40 °C. Moreover, the copolymerization rate was clearly lower when the content of  $\gamma\text{M}\gamma\text{BL}$  in the feed was higher. After 12 h. the conversion reached 36 %, 20 %, and 11 % for  $f_{\gamma\text{M}\gamma\text{BL}}^{\circ}$  equal to 0.2, 0.4, and 0.7, respectively (Table 2). This trend is obvious when considering the time dependence of the  $\ln[M]_0/[M]$  function (Figure 3a) for the three compositions. The molar fraction of  $\gamma\text{M}\gamma\text{BL}$  was systematically lower in the copolymer compared to the feed, as suggested by the reactivity

ratios ( $r_{\gamma\text{M}\gamma\text{BL}} = 0.2$ ,  $r_{\text{VAc}} = 1.05$ ). Note that the experimental  $F_{\gamma\text{M}\gamma\text{BL}}$  ( $F_{\gamma\text{M}\gamma\text{BL exp}} = 0.19, 0.33, \text{ and } 0.53$ ) were close to the prediction based on the reactivity ratios ( $F_{\gamma\text{M}\gamma\text{BL th}} = 0.17, 0.31, \text{ and } 0.50$ ). As an additional proof of the incorporation of  $\gamma\text{M}\gamma\text{BL}$  in the copolymers, the thermal degradation profile of the copolymers and their glass transition temperature ( $T_g$ ) differ from those of PVAc (Figure S5). Because of the incorporation of rigid lactones along the backbone of the P( $\gamma\text{M}\gamma\text{BL-co-VAc}$ ) copolymers,  $T_g$  increased from 31 °C for a homo-PVAc prepared by OMRP to 64, 77, and 83 °C for copolymers with  $F_{\gamma\text{M}\gamma\text{BL}}$  equal to 0.19, 0.33, and 0.53, respectively.

As illustrated in Figure 3b, the  $M_n$  of P( $\gamma\text{M}\gamma\text{BL-co-VAc}$ ) regularly increases with monomer conversion, suggesting the controlled character of the copolymerization. The shift of the SEC chromatograms of the samples withdrawn at different polymerization times is represented in Figure 3c. Moreover, the dispersities remained low ( $\mathcal{D} \approx 1.1\text{--}1.3$ ) until 30 % conversion but tended to broaden at a higher conversion, especially for the  $\gamma\text{M}\gamma\text{BL}$ -rich copolymers. The theoretical molar masses of the final copolymers are also shown in Table 2. The latter are calculated based on the monomer/initiator ratio, the conversion, and the composition of the copolymers. Note that  $M_{n \text{ exp}}$  was determined by SEC using a PS calibration, which might also account for the deviation from  $M_{n \text{ th}}$ . As expected for a controlled process, the P( $\gamma\text{M}\gamma\text{BL-co-VAc}$ ) molar mass also strongly depends on the comonomer/ initiator ratios. For a similar  $\gamma\text{M}\gamma\text{BL/VAc}$  molar ratio (2/8), P( $\gamma\text{M}\gamma\text{BL-co-VAc}$ )s with higher molar masses were obtained when increasing the [comonomer]/[PVAc-Co] ratio as illustrated in Figure S6 and Table S3.

Next, we took advantage of the controlled copolymerization of  $\gamma\text{M}\gamma\text{BL}$  and VAc for macromolecular engineering, in particular for the one-pot synthesis of PVAc-b-P( $\gamma\text{M}\gamma\text{BL-co-VAc}$ ) block copolymers. The general strategy consists in the sequential OMRP of VAc and  $\gamma\text{M}\gamma\text{BL/VAc}$  copolymerization (Figure 4). In practice, a well-defined PVAc-Co(acac)<sub>2</sub> precursor ( $M_{n \text{ SEC}} = 10000 \text{ g/mol}$ ,  $\mathcal{D} = 1.06$ ) prepared at 40 °C in bulk from PVAc<sub>4</sub>-Co(acac)<sub>2</sub> served as a macroinitiator for the  $\gamma\text{M}\gamma\text{BL/VAc}$  copolymerization ( $f_{\gamma\text{M}\gamma\text{BL}}^{\circ} = 0.2$ ) performed under the same experimental conditions. The overlay of the SEC chromatograms in Figure 4 confirms the efficiency of the chain extension as well as the controlled character of the synthesis of the statistical sequence. Indeed, the chromatogram corresponding to the PVAc macroinitiator was clearly shifted toward higher molar masses. It should be noted, however, that a tailing appeared on the low molar mass side of the peak probably because of bimolecular radical termination or chain-transfer reactions causing a broadening of the peaks beyond 30 % of monomer conversion. At this stage, we cannot exclude the fact that this broadening may also result from the difficulty to reactivate some inverted head-to-head  $\gamma\text{M}\gamma\text{BL}$  adducts. Nevertheless,  $\gamma\text{M}\gamma\text{BL}$ -containing block copolymers were successfully prepared for the first time.

Some interesting mechanistic conclusions can be drawn at this stage on the OMRP of  $\gamma\text{M}\gamma\text{BL}$ . All the abovementioned experiments were initiated with a preformed alkyl-cobalt(III) species in the absence of an additional radical source and therefore necessarily followed a reversible termination (RT) pathway,<sup>43,73,74</sup> which consists in the reversible homolytic rupture of the cobalt-carbon bond at the polymer chain end (Figure 5). In the case of the OMRP of VAc, the bond dissociation enthalpy of the PVAc-Co(acac)<sub>2</sub> model (species **2**) was estimated at 9.2 kcal/mol by density functional theory (DFT) calculations. Moreover, in the absence of coordinating molecules, the PVAc-Co(acac)<sub>2</sub> dormant species also benefits from the extrastabilization of 3.9 kcal/mol upon intramolecular chelation via the terminal ester unit of the PVAc chain (species **3**).<sup>43,73,74</sup> For the sake of comparison, we performed similar DFT calculations for  $\gamma\text{M}\gamma\text{BL}$ . The bond dissociation enthalpy of the model P $\gamma\text{M}\gamma\text{BL-Co(acac)}_2$  (species **2'**) was slightly higher compared to the PVAc-Co(acac)<sub>2</sub> one, namely 12.0 kcal/mol. However, the stabilization of the dormant P $\gamma\text{M}\gamma\text{BLCo(acac)}_2$  by intramolecular chelation of cobalt by the ester function unit is

hampered by the geometrical constraint of the lactone. The reorganization of the coordination sphere from square-pyramidal with an apical alkyl group to square-pyramidal with the apical position occupied by one O atom of one acac ligand, which is required to generate a cis vacant site for monomer chelation in species **3'**, is energetically costly (+15.1 kcal/mol) and cannot be compensated by the donation of the carbonyl oxygen electron density as in species **3**. Instead, only a slight interaction with the endocyclic oxygen atom may occur, as shown by the distortion imposed on the cobalt-bonded C atom configuration (Co–C–O = 84.1°; Co–C–C(H<sub>3</sub>) = 117.1°; Co–C–C(H<sub>2</sub>) = 117.6°). This interaction, however, is very weak (Co···O = 2.27 Å; cf. with the Co–O distance of 1.93 Å in the chelated VAc monomer in species **3**). Overall, the chelated PVAc-Co and nonchelated PγMγBL-Co (dormant species **3** and **2'**, respectively) exhibit quite similar global bond dissociation enthalpies (13.1 and 12.0 kcal/mol, respectively) and should efficiently reactivate under similar conditions, for example, in bulk at 40 °C. Consequently, the extremely low conversion for the homopolymerization of γMγBL by OMRP at 40 °C cannot result from a high PγMγBLCo(acac)<sub>2</sub> bond strength. It can rather be attributed to a low k<sub>p</sub> of γMγBL at this temperature. As a confirmation, no conversion was observed for the conventional radical homopolymerization of γMγBL at 40 °C (Table 1, entry 1). Concerning the OMRP of γMγBL at 70 °C, it is reasonable to assume that the PγMγBL-Co(acac)<sub>2</sub> bond is too weak to establish an appropriate equilibrium between dormant and active species at this temperature, leading to massive and premature termination of the radical chains and ultimately inhibition of the polymerization by the accumulation of the cobalt(II) deactivator in the polymerization medium. However, the successful organometallic-mediated radical copolymerization of VAc and γMγBL at 40 °C is fully consistent with similar C–Co bond strength for the VAc and γMγBL model dormant species. Under these conditions, both dormant species can reactivate and the terminal γMγBL radicals can further cross-propagate with VAc, leading to well-defined P(γMγBL-co-VAc) copolymers.

In addition to the RT pathway, OMRP is also known to proceed via a degenerative chain transfer (DT) mechanism, in which an active radical chain displaces the dormant chain bound to the metal via an associative exchange reaction.<sup>43,73,74</sup> This mode notably prevails in the absence of coordinating molecules and when an excess of radicals relative to cobalt is generated in the polymerization medium. In this case, the polymerization rate and radical concentration are close to those observed for conventional radical polymerizations. In practice, DT polymerizations are initiated from commercially available conventional radical initiators used in excess compared to the cobalt complex, preventing the synthesis of sensitive alkyl-cobalt(III) initiators. Both the homopolymerization of γMγBL and the γMγBL/VAc copolymerization were tested in the DT mode (Scheme 4).

In practice, the polymerization of γMγBL was performed in bulk in the presence of Co(acac)<sub>2</sub> and AIBN ([γMγBL]<sub>0</sub>/ [AIBN]<sub>0</sub>/ [Co(acac)<sub>2</sub>]<sub>0</sub> = 500/3/1) at 65 °C to ensure the formation of PγMγBL (Table S4, entry 1). Under these conditions, the conversion increased from 6 to 28 % between 3 and 24 h of reaction without significant evolution of the polymer molar mass (*M<sub>n</sub>* ≈ 7000 g/mol, *D* ≈ 1.6–1.8), indicating an uncontrolled polymerization process. On the other hand, inspired by previous reports on the OMRP of VAc by DT, the controlled copolymerization of γMγBL/VAc (*f*<sup>o</sup><sub>γMγBL</sub> = 0.2) was examined in the DT regime at 30 °C using three equivalents of V70 relative to Co(acac)<sub>2</sub> (Table S4, entry 2). Kinetics data and the molecular parameter (*M<sub>n</sub>*, *D*) dependence on the monomer conversion are plotted in Figure 6. In contrast to the γMγBL/VAc copolymerization initiated with the PVAc-Co(acac)<sub>2</sub> initiator and carried out under the RT regime, an induction period of several hours was observed in the DT mode (Figure 6b). As described elsewhere for the OMRP of VAc,<sup>43</sup> the induction period corresponds to the time needed to generate a sufficient amount of radicals for converting most of Co<sup>II</sup>(acac)<sub>2</sub> into the alkyl-cobalt(III)

dormant species. After this period, a controlled polymerization of  $\gamma$ M $\gamma$ BL and VAc was observed as suggested by the pseudofirst-order kinetics and the linear increase of the molar mass with the monomer conversion (Figure 6b) while maintaining a low dispersity ( $\mathcal{D} \approx 1.1\text{--}1.3$ ) (Figure 6a). Overall, this approach represents a straightforward route for the controlled synthesis of P( $\gamma$ M $\gamma$ BL-*co*-VAc)s involving readily available initiator and controlling agents.

### Postpolymerization Modification of $\gamma$ M $\gamma$ BL-Based (Co)polymers.

PVA is a major industrial polymer commonly prepared by the hydrolysis of poly(VAc).<sup>75–77</sup> The presence of one hydroxyl group per repeating unit makes it highly hydrophilic although PVA with a high level of hydrolysis exhibits limited water solubility because of the formation of regular hydrogen-bonding networks.<sup>45,75,78,79</sup> On the other hand, the literature is replete with examples of modified PVA produced by radical copolymerization of VAc with comonomers prior to hydrolysis or partial hydrolysis.<sup>77,80–83</sup> Both approaches disrupt the regular sequence of hydroxyl groups typical of PVA. In this respect, the hydrolysis of the  $\gamma$ M $\gamma$ BL containing (co)polymers prepared above should offer new functionalities to PVA without altering its characteristic hydroxyl sequence. Indeed, the hydrolysis of the pendant lactone ring should release one alcohol moiety and one carboxylic acid group within the same repeating unit (Scheme 5). This equals the modification of the PVA backbone at the methine position. Interestingly, decorating PVAs with carboxylic acid moieties should impart to them unique pH responsiveness. These were strong incentives to investigate the hydrolysis of both P $\gamma$ M $\gamma$ BL and P( $\gamma$ M $\gamma$ BL-*co*-VAc) and to carry out a preliminary study of its water solution properties.

A homo-P $\gamma$ M $\gamma$ BL (4200 g/mol,  $\mathcal{D} = 1.89$ ) and a P( $\gamma$ M $\gamma$ BL-*co*-VAc) (13800 g/mol,  $\mathcal{D} = 1.65$ ,  $F_{\gamma\text{M}\gamma\text{BL}} = 0.32$ ), prepared by conventional radical polymerization and OMRP, respectively, were subjected to basic hydrolysis. Typically, P $\gamma$ M $\gamma$ BL was treated with sodium hydroxide in an acetonitrile/water (1/1: v/v) mixture at room temperature for 48 h followed by dialysis against distilled water. Note that the water solubility of the treated polymer was a first indication of significant modification of the polymer structure. The successful hydrolysis of most of the pendant lactone ring of P $\gamma$ M $\gamma$ BL was further confirmed by IR (Figure S7b). Indeed, the IR spectrum shows a significant decrease of the characteristic signals of the ester units (C = O ester) at 1759  $\text{cm}^{-1}$  and the appearance of a large band at 3300  $\text{cm}^{-1}$ , typical of the hydroxyl moieties, as well as an intense peak at 1556  $\text{cm}^{-1}$  assigned to the carboxylate groups. <sup>1</sup>H NMR in D<sub>2</sub>O of the treated P $\gamma$ M $\gamma$ BL, namely poly(4-hydroxypent-4-enoic acid) (PHPEA), also supports the successful hydrolysis of lactones (Figure 7a). Indeed, a signal corresponding to methylene protons **b** at the alpha position of the carboxyl group appeared at 2.20 ppm. Note that some residual lactone (10 %) was detected at 2.65 ppm. The structure of the hydrolyzed P $\gamma$ M $\gamma$ BL was also corroborated by COSY and HSQC (Figure S8). The P( $\gamma$ M $\gamma$ BL-*co*-VAc) copolymer (13800 g/mol,  $\mathcal{D} = 1.65$ ,  $F_{\gamma\text{M}\gamma\text{BL}} = 0.32$ ) was treated with sodium hydroxide in a THF/water (1/1: v/v) mixture at room temperature for 48 h, leading to the corresponding modified PVA copolymer via hydrolysis of both lactones and acyclic pendant esters, as confirmed by IR (Figure S7d) and <sup>1</sup>H NMR (Figure 7b). In addition to the peak at 2.20 ppm corresponding to the methylene protons **e**, namely the alpha position of the carboxyl group in the hydrolyzed  $\gamma$ M $\gamma$ BL units, we also observed characteristic signals of the vinyl alcohol units, namely the methine protons **b** around 4 ppm. In this case, 3 % of unmodified lactone was detected at 2.65 ppm. The COSY and HSQC spectra of the P(HPEA-*co*-VA) copolymer are provided in the Supporting Information (Figure S9).

Finally, we carried out a preliminary study of the aqueous solution properties of the PHPEA and P(HPEA-*co*-VA) ( $F_{\text{HPEA}} = 0.32$ ) (co)polymers prepared above. Given the presence of the carboxylic group

along their backbone, special care was devoted to their possible pH responsiveness. As illustrated in Figure 8, both PHPEA and P(HPEA-*co*-VA) were fully soluble in water at pH 7 (at 5 mg/mL). Under these conditions, the pendant carboxylic acid groups are deprotonated, which favors the (co)polymer solubilization. However, drastic changes occurred upon acidification of the solution to pH 1. Indeed, PHPEA clearly precipitates after protonation of its carboxylic acid groups leading to the formation of rather large particles, as emphasized by dynamic light scattering (DLS) (mean diam > 2  $\mu\text{m}$ ). In contrast, the aqueous solution of P(HPEA-*co*-VA) did not turn opaque when acidified to pH 1; rather, it became slightly turbid, suggesting the formation of smaller objects. In addition to few large aggregates, DLS emphasized the formation of objects with an average diameter of 550 nm. Compared to PHPEA, which exhibits one pH-sensitive carboxylic acid function per repeating unit, P(HPEA-*co*-VA) presents a higher hydroxyl/carboxylic acid molar ratio which favored the stabilization of the submicron objects at low pH. Note that the transition occurred around pH 2.2 and was fully reversible for more than seven acidification/basification cycles, as illustrated in Figure S10.

## CONCLUSIONS

The use of nonconjugated lactones in conventional and reversible deactivation radical polymerizations has previously been largely overlooked. In this report, we have shown the potential of  $\gamma\text{M}\gamma\text{BL}$  as a monomer and comonomer in combination with VAc in radical polymerization processes.

Poly( $\gamma\text{M}\gamma\text{BL}$ ) was successfully produced by the conventional radical polymerization of  $\gamma\text{M}\gamma\text{BL}$  at 70 °C, whereas no polymer formed at 40 °C because of a low propagation rate constant under these conditions. However, attempts to polymerize  $\gamma\text{M}\gamma\text{BL}$  via OMRP based on  $\text{Co}(\text{acac})_2$  failed. This results from the difficulty to find a temperature window which guarantees a sufficient propagation rate constant and ensures a proper equilibrium between active and dormant species, limiting irreversible termination reactions.

In contrast, the conventional radical copolymerization of  $\gamma\text{M}\gamma\text{BL}$  and VAc, its acyclic analogue, proceeded well at 40 °C. This paved the way to their controlled  $\text{Co}(\text{acac})_2$ -mediated radical copolymerization, following an RT pathway, at this temperature using a preformed alkyl-cobalt(III) initiator. A series of P( $\gamma\text{M}\gamma\text{BL}$ -*co*-VAc) with specific molar masses, low and moderate dispersities ( $\mathcal{D} \approx 1.2$ – $1.4$ ), and various compositions were produced accordingly. The reactivity ratios were measured by three methods, that is, FR, KT, and the nonlinear approach, leading to similar values, that is,  $r_{\gamma\text{M}\gamma\text{BL}} = 0.20$  and  $r_{\text{VAc}} = 1.05$ . These numbers confirmed the low propensity of  $\gamma\text{M}\gamma\text{BL}$  to self-propagate at 40 °C and the possibility to copolymerize it with VAc. The distribution of  $\gamma\text{M}\gamma\text{BL}$  along the copolymer chains was also evaluated by the Skeist model, revealing a rather homogeneous incorporation of vinyl lactone in the copolymer at least until 60 % conversion. DFT calculations confirmed that the model dormant species, namely  $\gamma\text{M}\gamma\text{BL-Co}(\text{acac})_2$  and  $\text{VAc-Co}(\text{acac})_2$ , have quite similar bond dissociation enthalpies, which limits the accumulation of one or the other dormant form in the polymerization medium and favors a controlled process. Interestingly, the controlled copolymerization of  $\gamma\text{M}\gamma\text{BL}$  and VAc was also achieved via degenerative chain-transfer mechanism starting from commercially available compounds, that is, V70 and  $\text{Co}(\text{acac})_2$ . In addition to controlling the overall composition and the comonomer sequence of the copolymers, mediating the  $\gamma\text{M}\gamma\text{BL/VAc}$  radical copolymerization opens several macromolecular engineering opportunities as emphasized by the synthesis of PVAc-*b*-P( $\gamma\text{M}\gamma\text{BL}$ -*co*-VAc) diblock copolymers.

Last but not least, P $\gamma$ M $\gamma$ BL and P( $\gamma$ M $\gamma$ BL-*co*-VAc) were converted into PHPEA and P(HPEA-*co*-VA), respectively, via ester hydrolysis under basic conditions. The  $\gamma$ M $\gamma$ BL units have the particularity to generate one alcohol moiety and one carboxylic acid group on the same chain C atom, giving access to unprecedented carboxylic acid-functionalized PVA without alteration of its characteristic hydroxyl sequence. The pH responsiveness of both (PHPEA) and P(HPEA-*co*-VA) in water was also demonstrated.

All these results support our initial idea that nonconjugated lactones like  $\gamma$ M $\gamma$ BL are promising building blocks for macromolecular engineering based on LAMs and for the design of unique functional and responsive materials.

## ASSOCIATED CONTENT

Supporting Information

The Supporting Information is available free of charge on the ACS Publications website at DOI: 10.1021/acs.macromol.9b01838.

Additional data, DFT calculations, SEC, NMR, DSC, and TGA characterizations (PDF)

## AUTHOR INFORMATION

ORCID

Rinaldo Poli: [0000-0002-5220-2515](https://orcid.org/0000-0002-5220-2515)

Antoine Debuigne: [0000-0002-7909-7006](https://orcid.org/0000-0002-7909-7006)

Notes

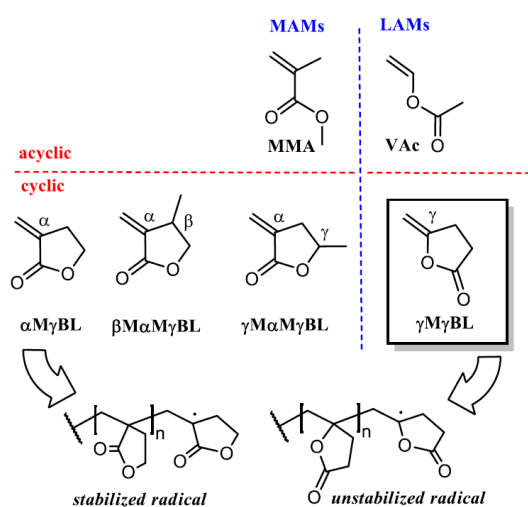
The authors declare no competing financial interest.

## ACKNOWLEDGMENTS

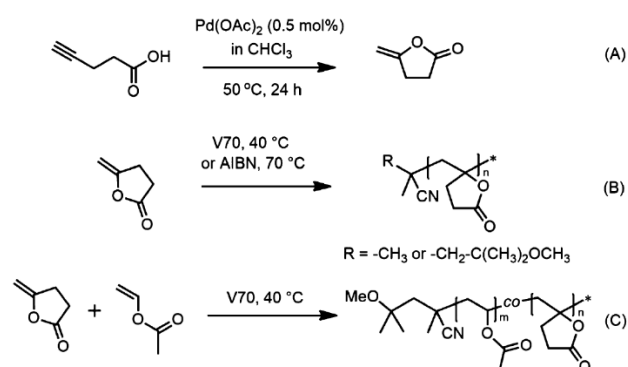
The authors from Liege thank the Fonds de la Recherche Scientifique (FNRS) and the Fonds Wetenschappelijk Onderzoek–Vlaanderen (FWO) for funding the EOS project no. 0019618F (ID EOS: 30902231) and the NECOPOL project (convention U.N054.17). A.D. and C.D. are Research Associate and Research Director by F.R.S.–FNRS, respectively. The authors are grateful to the CALMIP mesocenter of the University of Toulouse for the allocation of computational resources.

## Schemes

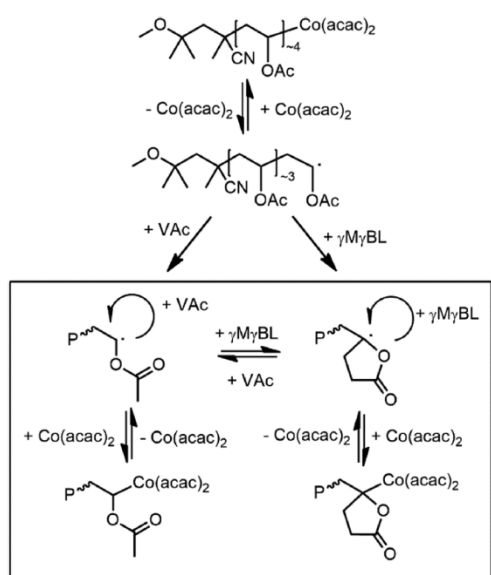
**Scheme 1.** Radical Polymerization of Conjugated and Nonconjugated Methylene- $\gamma$ -butyrolactones



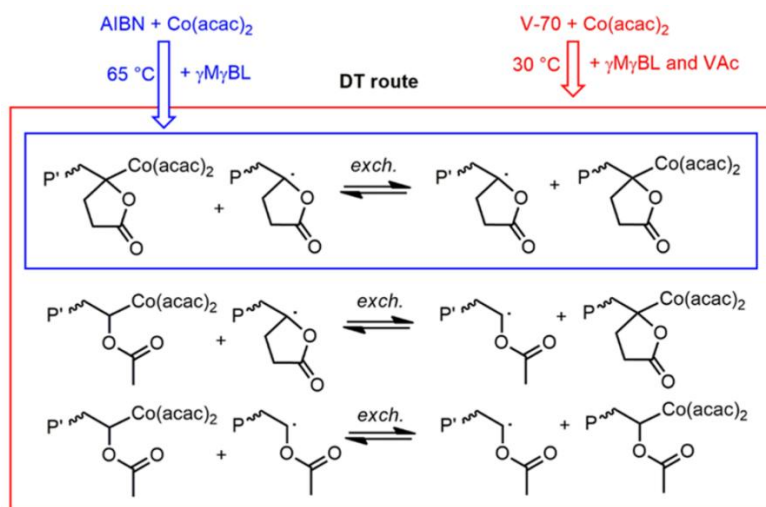
**Scheme 2.** Synthesis and Conventional Radical (Co)polymerization of  $\gamma$ M $\gamma$ BL



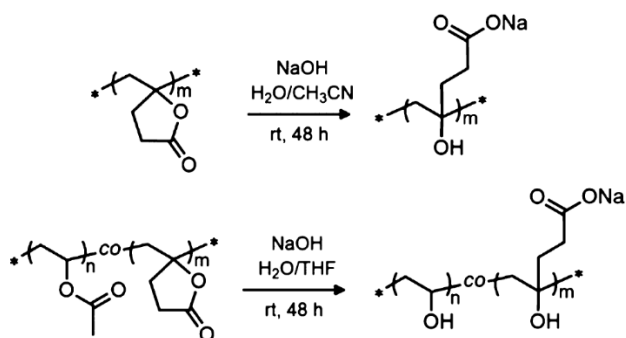
**Scheme 3.** Organometallic-Mediated Radical Copolymerization of  $\gamma$ M $\gamma$ BL and Vac



**Scheme 4.** Mechanism of the Homopolymerization of  $\gamma$ M $\gamma$ BL and the  $\gamma$ M $\gamma$ BL/VAc Copolymerization via OMRP in the DT Mode



**Scheme 5.** Hydrolysis of P $\gamma$ M $\gamma$ BL and P( $\gamma$ M $\gamma$ BL-co-VAc)



## Tables

**Table 1.** Conventional Radical (Co)polymerization of  $\gamma$ M $\gamma$ BLa

entry	initiator/temp	$f_{\gamma\text{M}\gamma\text{BL}}^{\circ}$	$f_{\text{VAc}}^{\circ}$	conv. (%)		$M_{n \text{ SEC}}$ (g/mol)	$\bar{D}$	$F_{\gamma\text{M}\gamma\text{BL}}$
				$\gamma\text{M}\gamma\text{BL}$	VAc			
1	V70/40 °C	1	0	<1 <sup>b</sup>	NA			
2	AIBN/70 °C	1	0	41 <sup>b</sup>	NA	4200 <sup>d</sup>	1.89 <sup>df</sup>	1.00
3	V70/40 °C	0.20	0.80	66 <sup>c</sup>	75	12 000 <sup>e</sup>	2.24 <sup>c</sup>	0.19 <sup>f</sup>
4	V70/40 °C	0.40	0.60	54 <sup>c</sup>	57	8100 <sup>e</sup>	2.01 <sup>e</sup>	0.32 <sup>f</sup>

<sup>a</sup>Conditions: bulk polymerization, 24 h, 5 mol % of azoinitiator vs monomer(s). <sup>b</sup>Determined by gravimetry. <sup>c</sup>Determined by <sup>1</sup>H NMR in CDCl<sub>3</sub>. <sup>d</sup>Determined by SEC<sub>DMF cal PS</sub>. <sup>e</sup>Determined by SEC<sub>THF cal PS</sub>. <sup>f</sup>Determined by <sup>1</sup>H NMR in CDCl<sub>3</sub>.

**Table 2.** Organometallic-Mediated Radical (Co)polymerization of  $\gamma$ M $\gamma$ BL and Vaca

entry	$f_{\gamma\text{M}\gamma\text{BL}}^{\circ}$	$f_{\text{VAc}}^{\circ}$	time (h)	conv (%) <sup>b</sup>	$M_{n \text{ SEC}}$ (g/mol) <sup>c</sup>	$\bar{D}$ <sup>c</sup>	$F_{\gamma\text{M}\gamma\text{BL}}$ <sup>b</sup>	$M_{n \text{ th}}$ (g/mol) <sup>e</sup>
1	0.20	0.80	2	7	5200	1.10		
			4	15	6600	1.17		
			6	21	7900	1.22		
			8	27	8500	1.28		
			10	32	9400	1.32		
			12	36	10200	1.33	0.19	15 900
2	0.40	0.60	3	6	4000	1.13		
			6	11	5700	1.16		
			9	15	6900	1.22		
			12	20	8000	1.28		
			15	25	8400	1.36		
			30	35	12000	1.56	0.33	15 800
3	0.70	0.30	3	4	4400	1.19		
			6	6	5900	1.25		
			9	9	6900	1.36		
			12	11	7900	1.43		
			30	20	9500 <sup>d</sup>	1.63 <sup>d</sup>	0.53	9200

<sup>a</sup>Conditions: 40 °C, [monomer]/[RCo] = 500. <sup>b</sup>Total monomer conversion determined by <sup>1</sup>H NMR in CDCl<sub>3</sub>. <sup>c</sup>Determined by SEC in THF using a PS calibration. <sup>d</sup>Determined by SEC in DMF/LiBr using a PS calibration because of the low solubility of this sample in THF. <sup>e</sup>Theoretical molar mass ( $M_{n \text{ th}}$ ) calculated based on the [monomer]/[RCo] ratio, the conversion, and the composition of the copolymer.

## Figures

**Figure 1.**  $^1\text{H}$  NMR of  $P\gamma\text{MyBL}$  (a) and  $P(\gamma\text{MyBL-co-VAc})$  ( $f_{\gamma\text{MyBL}}^0 = 0.32$ ) (b) in  $\text{CD}_3\text{CN}$  and  $\text{CDCl}_3$ , respectively.

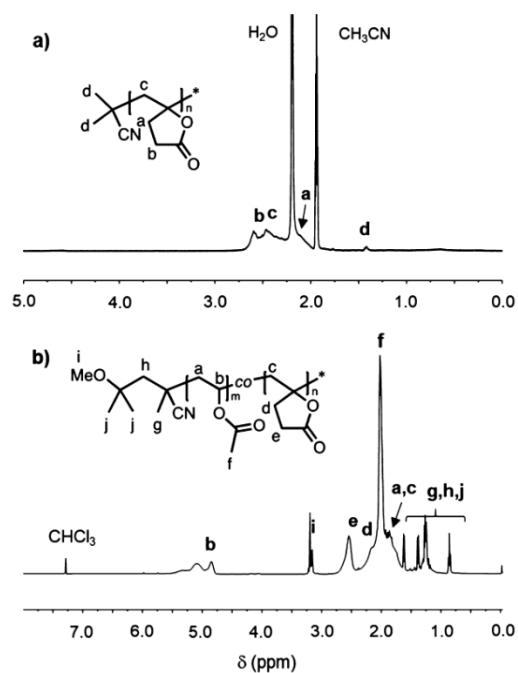


**Figure 2.** Determination of the reactivity ratios for the radical copolymerization of  $\gamma\text{MyBL}$  and  $\text{VAc}$  in bulk at  $40^\circ\text{C}$  by three methods: FR (a), KT (b), and the nonlinear least-squares fitting method based on the Mayo Lewis equation (c). Experimental data are presented in Table S1. (d) Evolution of the instantaneous molar fraction in the feed ( $f_{\gamma\text{MyBL}}$ ) and also of the cumulative ( $F_{\gamma\text{MyBL}}$ ) and instantaneous ( $F_{\text{inst } \gamma\text{MyBL}}$ ) molar fractions of comonomers in the copolymer with the overall molar monomer conversion for an initial  $\gamma\text{MyBL}$  feed ratio of 0.4 ( $f_{\gamma\text{MyBL}}^0$ ). Compositions are calculated based on Skeist's model.

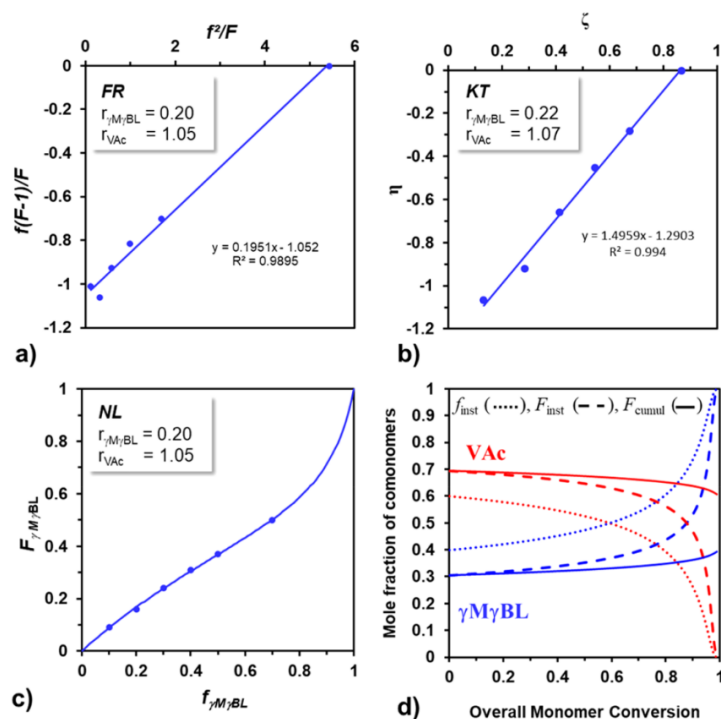


**Figure 3.** (a) Time dependence of  $\ln[M]_0/[M]$  and (b) dependence of  $M_n$  (full symbols) and  $\bar{D}$  (hollow symbols) on the total monomer conversion for the OMRP of  $\gamma$ MyBL and VAc with different compositions:  $f^{\circ}_{\gamma\text{MyBL}} = 0.2$  ( $\bullet$ ),  $0.4$  ( $\blacktriangle$ ), and  $0.7$  ( $\blacksquare$ ) (see Table 2 for detailed conditions). (c) Overlay of SEC traces for the OMRP of  $\gamma$ MyBL and VAc ( $f^{\circ}_{\gamma\text{MyBL}} = 0.2$ , Table 2 entry 1).

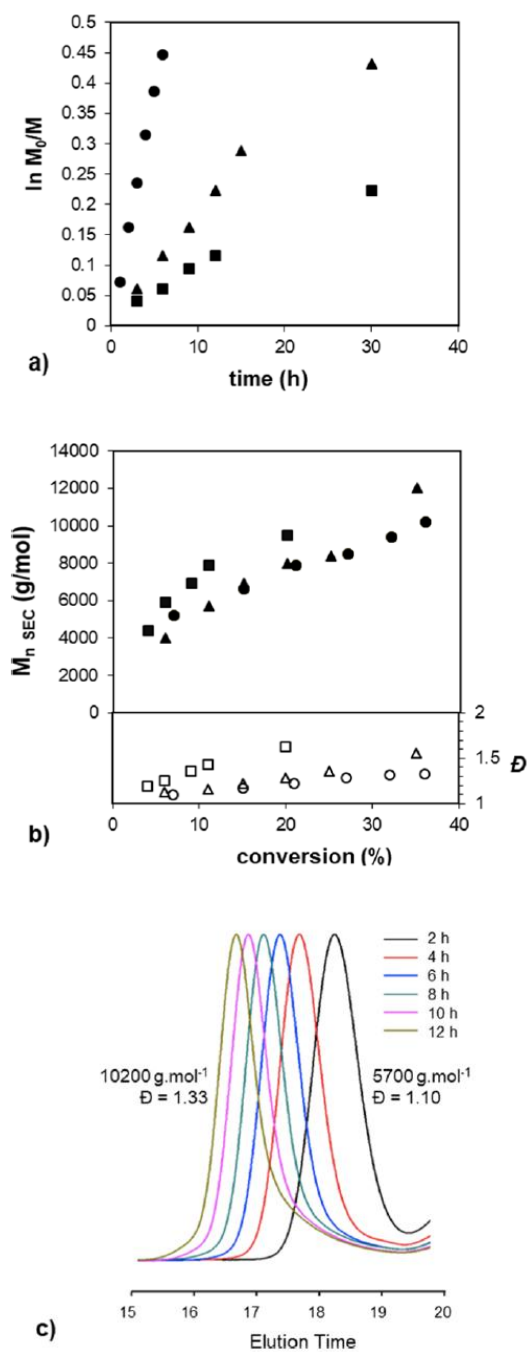


**Figure 4.** General strategy for the synthesis of  $\gamma$ MyBL-containing block copolymers by OMRP and overlay of the SEC chromatograms for the homoPVAc-Co(acac)<sub>2</sub> precursor and the resulting PVAc-b-P( $\gamma$ MyBL-co-VAc) deblocks.

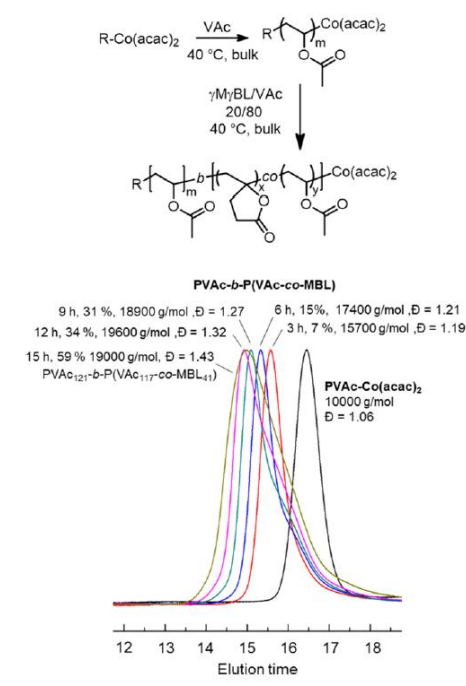


**Figure 5.** DFT calculation of the bond dissociation enthalpies for the  $\gamma$ MyBL-Co(acac)<sub>2</sub> and VAc-Co(acac)<sub>2</sub> model species.

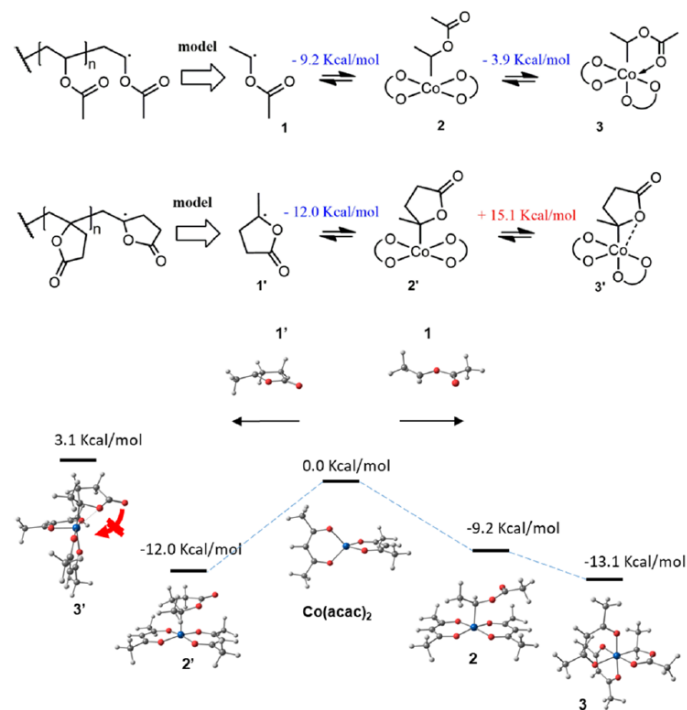


**Figure 6.** (a) Time dependence of  $\ln[M]_0/[M]$  and (b) dependence of  $M_n$  and  $\bar{D}$  on the monomer conversion for the OMRP of  $\gamma$ M $\gamma$ BL and VAc via RT (●) or DT (■). Conditions: (●)  $[VAc]_0/[ \gamma M \gamma BL ]_0/[PVAc_4-Co(acac)_2]_0 = 400/100/1$ , 40 °C; (■)  $[VAc]_0/[ \gamma M \gamma BL ]_0/[V70]_0/[Co(acac)_2]_0 = 400/100/3/1$ , 30 °C.

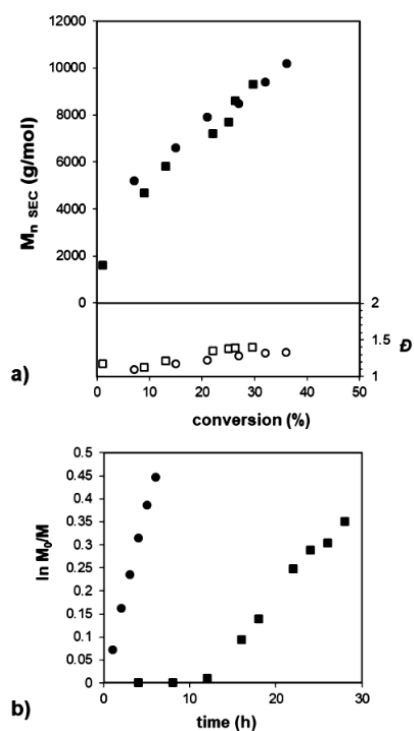


**Figure 7.**  $^1H$  NMR spectra in  $D_2O$  after hydrolysis of (a) PHPEA and (b) P(HPEA-co-VA) obtained by hydrolysis of P $\gamma$ M $\gamma$ BL (4200 g/mol,  $\bar{D}$  = 1.89) and a P( $\gamma$ M $\gamma$ BL-co-VAc) (13800 g/mol,  $\bar{D}$  = 1.65,  $F_{\gamma M \gamma BL}$  = 0.32), respectively.

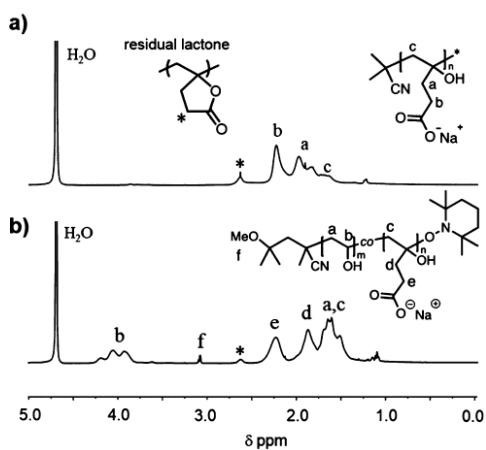
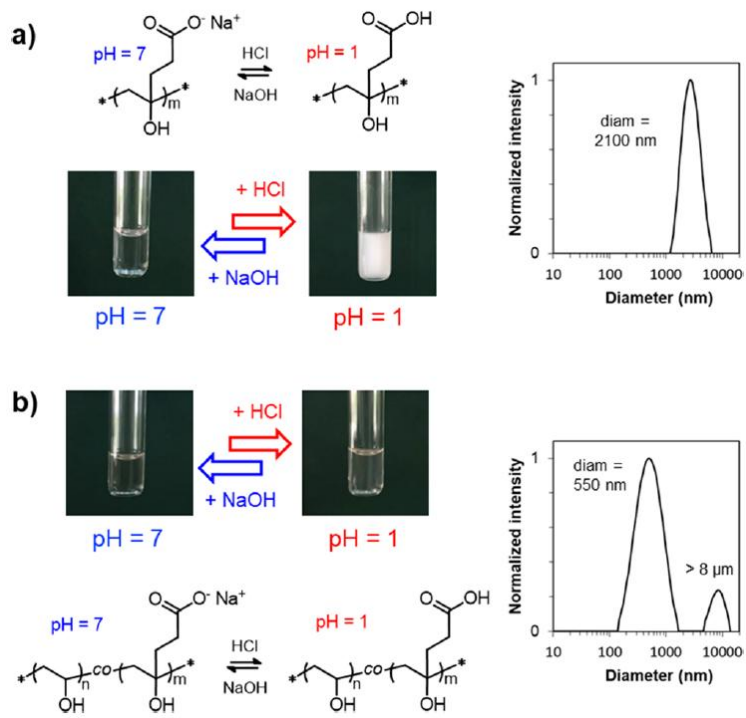


**Figure 8.** Illustration of the aqueous solution behavior and pH responsiveness of (a) PHPEA and (b) P(HPEA-co-VA) at room temperature at 5 mg/mL.



## REFERENCES

- (1) Gowda, R. R.; Chen, E. Y.-X. Sustainable Polymers from Biomass-Derived  $\alpha$ -Methylene- $\gamma$ -Butyrolactones. *Encyclopedia of Polymer Science and Technology*, 4th ed.; Wiley, 2014; Vol. 8, pp 235–271.
- (2) Gowda, R. R.; Chen, E. Y.-X. Synthesis of  $\beta$ -methyl- $\alpha$ -methylene- $\gamma$ -butyrolactone from biorenewable itaconic acid. *Org. Chem. Front.* 2014, 1, 230–234.
- (3) Manzer, L. E. Catalytic Synthesis of  $\alpha$ -Methylene- $\gamma$ -Valerolactone : a Biomass-Derived Acrylic Monomer. *Appl. Catal., A* 2004, 272, 249–256.
- (4) Tang, X.; Hong, M.; Falivene, L.; Caporaso, L.; Cavallo, L.; Chen, E. Y.-X. The Quest for Converting Biorenewable Bifunctional  $\alpha$ -Methylene- $\gamma$ -butyrolactone into Degradable and Recyclable Polyester: Controlling Vinyl-Addition/Ring-Opening/Cross-Linking Pathways. *J. Am. Chem. Soc.* 2016, 138, 14326–14337.
- (5) Hong, M.; Chen, E. Y.-X. Coordination Ring-Opening Copolymerization of Naturally Renewable  $\alpha$ -Methylene- $\gamma$ -butyrolactone into Unsaturated Polyesters. *Macromolecules* 2014, 47, 3614–3624.
- (6) Danko, M.; Basko, M.; Ďurkáčová, S.; Duda, A.; Mosnáček, J. Functional Polyesters with Pendant Double Bonds Prepared by Coordination-Insertion and Cationic Ring-Opening Copolymerizations of  $\epsilon$ -Caprolactone with Renewable Tulipalin A. *Macromolecules* 2018, 51, 3582–3596.
- (7) Miyake, G. M.; Zhang, Y.; Chen, E. Y.-X. Living Polymerization of Naturally Renewable Butyrolactone-Based Vinylidene Monomers by Ambiphilic Silicon Propagators. *Macromolecules* 2010, 43, 4902–4908.
- (8) Hu, L.; He, J.; Zhang, Y.; Chen, E. Y.-X. Living Group Transfer Polymerization of Renewable  $\alpha$ -Methylene- $\gamma$ -butyrolactones Using  $Al(C_6F_5)_3$  Catalyst. *Macromolecules* 2018, 51, 1296–1307.
- (9) Hu, Y.; Gustafson, L. O.; Zhu, H.; Chen, E. Y.-X. Anionic Polymerization of MMA and Renewable Methylene Butyrolactones by Resorbable Potassium Salts. *J. Polym. Sci., Part A: Polym. Chem.* 2011, 49, 2008–2017.
- (10) Zhang, Y.; Miyake, G. M.; Chen, E. Y.-X. Alane-Based Classical and Frustrated Lewis Pairs in Polymer Synthesis: Rapid Polymerization of MMA and Naturally Renewable Methylene Butyrolactones into High-Molecular-Weight Polymers. *Angew. Chem., Int. Ed.* 2010, 49, 10158–10162.
- (11) Zhang, Y.; Miyake, G. M.; John, M. G.; Falivene, L.; Caporaso, L.; Cavallo, L.; Chen, E. Y.-X. Lewis Pair Polymerization by Classical and Frustrated Lewis Pairs: Acid, Base and Monomer Scope and Polymerization Mechanism. *Dalton Trans.* 2012, 41, 9119.
- (12) Chen, J.; Chen, E. Reactivity of Amine/ $E(C_6F_5)_3$  ( $E = B, Al$ ) Lewis Pairs toward Linear and Cyclic Acrylic Monomers: Hydrogenation vs. Polymerization. *Molecules* 2015, 20, 9575–9590.
- (13) Zhang, Y.; Schmitt, M.; Falivene, L.; Caporaso, L.; Cavallo, L.; Chen, E. Y. Organocatalytic Conjugate-Addition Polymerization of Linear and Cyclic Acrylic Monomers by  $N$ -Heterocyclic Carbenes: Mechanisms of Chain Initiation, Propagation, and Termination. *J. Am. Chem. Soc.* 2013, 135, 17925–17942.
- (14) He, J.; Zhang, Y.; Falivene, L.; Caporaso, L.; Cavallo, L.; Chen, E. Y.-X. Chain Propagation and Termination Mechanisms for Polymerization of Conjugated Polar Alkenes by  $[Al]$ -Based Frustrated Lewis Pairs. *Macromolecules* 2014, 47, 7765–7774.
- (15) Chen, X.; Caporaso, L.; Cavallo, L.; Chen, E. Y.-X. Stereoselectivity in Metallocene-Catalyzed Coordination Polymerization of Renewable Methylene Butyrolactones: From Stereo-random to Stereo-perfect Polymers. *J. Am. Chem. Soc.* 2012, 134, 7278–7281.

- (16) Miyake, G. M.; Newton, S. E.; Mariott, W. R.; Chen, E. Y.-X. Coordination Polymerization of Renewable Butyrolactone-Based Vinyl Monomers by Lanthanide and Early Metal Catalysts. *Dalton Trans.* 2010, 39, 6710–6718.
- (17) Hu, Y.; Wang, X.; Chen, Y.; Caporaso, L.; Cavallo, L.; Chen, E. Y.-X. Rare-Earth Half-Sandwich Dialkyl and Homoleptic Trialkyl Complexes for Rapid and Stereoselective Polymerization of a Conjugated Polar Olefin. *Organometallics* 2013, 32, 1459–1465.
- (18) Hu, Y.; Xu, X.; Zhang, Y.; Chen, Y.; Chen, E. Y.-X. Polymerization of Naturally Renewable Methylene Butyrolactones by Half-Sandwich Indenyl Rare Earth Metal Dialkyls with Exceptional Activity. *Macromolecules* 2010, 43, 9328–9336.
- (19) Akkapeddi, M. K. Poly( $\alpha$ -methylene- $\gamma$ -butyrolactone) Synthesis, Configurational Structure, and Properties. *Macromolecules* 1979, 12, 546–551.
- (20) Vobecka, Z.; Wei, C.; Tauer, K.; Esposito, D. Poly( $\alpha$ -methylene- $\gamma$ -valerolactone) 1. Sustainable monomer synthesis and radical polymerization studies. *Polymer* 2015, 74, 262–271.
- (21) Pittman, C. U.; Lee, H. Radical-Initiated Polymerization of  $\beta$ -Methyl- $\alpha$ -Methylene- $\gamma$ -Butyrolactone. *J. Polym. Sci., Part A: Polym. Chem.* 2003, 41, 1759–1777.
- (22) Akkapeddi, M. K. The free radical copolymerization characteristics of  $\alpha$ -methylene  $\gamma$ -butyrolactone. *Polymer* 1979, 20, 1215–1216.
- (23) Yoon, K.; Jung, D.; Lee, S.; Lee, S.; Choi, S.; Woo, S.; Moon, J. Novel 193nm Photoresist Based on Olefin-Containing Lactones. *Proceedings of the SPIE*, 2001; Vol. 4345, pp 688–694.
- (24) Cockburn, R. A.; Siegmann, R.; Payne, K. A.; Beuermann, S.; Mckenna, T. F. L.; Hutchinson, R. A. Free Radical Copolymerization Kinetics of  $\gamma$ -Methyl- $\alpha$ -methylene- $\gamma$ -butyrolactone (MeMBL). *Biomacromolecules* 2011, 12, 2319–2326.
- (25) Miyake, G. M.; Zhang, Y.; Chen, E. Y.-X. Polymerizability of Exo-methylene-lactide toward vinyl addition and ring opening. *J. Polym. Sci., Part A: Polym. Chem.* 2015, 53, 1523–1532.
- (26) Brandenburg, C. J. Graft Copolymers of Methylene Lactones and Process for Emulsion Polymerization of Methylene Lactones. U.S. Patent 6,841,627 (B2), 2005.
- (27) Kollár, J.; Mrlík, M.; Moravčíková, D.; Kroneková, Z.; Liptaj, T.; Lacík, I.; Mosnáček, J. Tulips: A Renewable Source of Monomer for Superabsorbent Hydrogels. *Macromolecules* 2016, 49, 4047–4056.
- (28) Ramram, M. B.; Chen, D.; Ma, Y.; Wang, L.; Yang, W. Stabilizer-free precipitation copolymerization of renewable bio-based  $\alpha$ -methylene- $\gamma$ -butyrolactone and styrene. *J. Macromol. Sci., Part A: Pure Appl. Chem.* 2016, 53, 484–491.
- (29) Moreno, M.; Goikoetxea, M.; de la Cal, J. C.; Barandiaran, M. J. From Fatty Acid and Lactone Biobased Monomers Toward Fully Renewable Polymer Latexes. *J. Polym. Sci., Part A: Polym. Chem.* 2014, 52, 3543–3549.
- (30) Mosnáček, J.; Matyjaszewski, K. Atom Transfer Radical Polymerization of Tulipalin A: A Naturally Renewable Monomer. *Macromolecules* 2008, 41, 5509–5511.
- (31) Mosnáček, J.; Yoon, J. A.; Juhari, A.; Koynov, K.; Matyjaszewski, K. Synthesis, Morphology and Mechanical Properties of Linear Triblock Copolymers Based on Poly( $\alpha$ -Methylene- $\gamma$ -Butyrolactone). *Polymer* 2009, 50, 2087–2094.
- (32) Juhari, A.; Mosnáček, J.; Yoon, J. A.; Nese, A.; Koynov, K.; Kowalewski, T.; Matyjaszewski, K. Star-like poly (*n*-butyl acrylate)-*b*-poly ( $\alpha$ -methylene- $\gamma$ -butyrolactone) block copolymers for high temperature thermoplastic elastomers applications. *Polymer* 2010, 51, 4806–4813.

- (33) Ding, K.; John, A.; Shin, J.; Lee, Y.; Quinn, T.; Tolman, W. B.; Hillmyer, M. A. High-Performance Pressure-Sensitive Adhesives from Renewable Triblock Copolymers. *Biomacromolecules* 2015, 16, 2537–2539.
- (34) Higaki, Y.; Okazaki, R.; Takahara, A. Semirigid Biobased Polymer Brush: Poly( $\alpha$ -methylene- $\gamma$ -butyrolactone) Brushes. *ACS Macro Lett.* 2012, 1, 1124–1127.
- (35) Trotta, J. T.; Jin, M.; Stawiasz, K. J.; Michaudel, Q.; Chen, W.L.; Fors, B. P. Synthesis of Methylene Butyrolactone Polymers from Itaconic Acid. *J. Polym. Sci., Part A: Polym. Chem.* 2017, 55, 2730–2737.
- (36) Qi, G.; Nolan, M.; Schork, F. J.; Jones, C. W. Emulsion and controlled miniemulsion polymerization of the renewable monomer  $\gamma$ -methyl- $\alpha$ -methylene- $\gamma$ -butyrolactone. *J. Polym. Sci., Part A: Polym. Chem.* 2008, 46, 5929–5944.
- (37) Xu, S.; Huang, J.; Xu, S.; Luo, Y. RAFT *ab initio* emulsion copolymerization of  $\gamma$ -methyl- $\alpha$ -methylene- $\gamma$ -butyrolactone and styrene. *Polymer* 2013, 54, 1779–1785.
- (38) Debuigne, A.; Jérôme, C.; Detrembleur, C. Organometallic-mediated radical polymerization of “less activated monomers”: Fundamentals, challenges and opportunities. *Polymer* 2017, 115, 285–307.
- (39) Poli, R. New phenomena in organometallic-mediated radical polymerization (OMRP) and perspectives for control of less active monomers. *Chem.–Eur. J.* 2015, 21, 6988–7001.
- (40) Hurtgen, M.; Detrembleur, C.; Jerome, C.; Debuigne, A. Insight into Organometallic-Mediated Radical Polymerization. *Polym. Rev.* 2011, 51, 188–213.
- (41) Demarteau, J.; Debuigne, A.; Detrembleur, C. Organocobalt Complexes as Sources of Carbon-Centered Radicals for Organic and Polymer Chemistries. *Chem. Rev.* 2019, 119, 6906–6955.
- (42) Debuigne, A.; Caille, J.-R.; Jérôme, R. Highly efficient cobalt-mediated radical polymerization of vinyl acetate. *Angew. Chem., Int. Ed.* 2005, 44, 1101–1104.
- (43) Debuigne, A.; Champouret, Y.; Jérôme, R.; Poli, R.; Detrembleur, C. Mechanistic insights into the cobalt-mediated radical polymerization (CMRP) of vinyl acetate with cobalt(III) adducts as initiators. *Chem.–Eur. J.* 2008, 14, 4046–4059.
- (44) Morin, A. N.; Detrembleur, C.; Jérôme, C.; De Tullio, P.; Poli, R.; Debuigne, A. Effect of head-to-head addition in vinyl acetate controlled radical polymerization: why is Co(acac)<sub>2</sub>-mediated polymerization so much better? *Macromolecules* 2013, 46, 4303–4312.
- (45) Drean, M.; Guégan, P.; Detrembleur, C.; Jérôme, C.; Rieger, J.; Debuigne, A. Controlled synthesis of poly(vinylamine)-based copolymers by organometallic-mediated radical polymerization. *Macromolecules* 2016, 49, 4817–4827.
- (46) Stiernet, P.; Drean, M.; Jérôme, C.; Midoux, P.; Guégan, P.; Rieger, J.; Debuigne, A. Tailor-Made Poly(vinylamine)s via Thermal or Photochemical Organometallic Mediated Radical Polymerization. *ACS Symposium Series*, 2018; Vol. 1284, pp 17–349.
- (47) Drean, M.; Debuigne, A.; Goncalves, C.; Jérôme, C.; Midoux, P.; Rieger, J.; Guégan, P. Use of Primary and Secondary Polyvinyl- amines for Efficient Gene Transfection. *Biomacromolecules* 2017, 18, 440–451.
- (48) Debuigne, A.; Morin, A. N.; Kermagoret, A.; Piette, Y.; Detrembleur, C.; Jérôme, C.; Poli, R. Key Role of Intramolecular Metal Chelation and Hydrogen Bonding in the Cobalt-Mediated Radical Polymerization of *N*-Vinyl Amides. *Chem.–Eur. J.* 2012, 18, 12834–12844.
- (49) Scholten, P. B. V.; Demarteau, J.; Gennen, S.; De Winter, J.; Grignard, B.; Debuigne, A.; Meier, M. A. R.; Detrembleur, C. Merging CO<sub>2</sub>-based building blocks with cobalt-mediated radical polymerization for the synthesis of functional poly(vinyl alcohol)s. *Macromolecules* 2018, 51, 3379–3393.

- (50) Scholten, P. B. V.; Detrembleur, C.; Meier, M. A. R. *PlantBased Nonactivated Olefins: A New Class of Renewable Monomers for Controlled Radical Polymerization*. *ACS Sustainable Chem. Eng.* 2019, 7, 2751–2762.
- (51) Piette, Y.; Debuigne, A.; Jérôme, C.; Bodart, V.; Poli, R.; Detrembleur, C. *Cobalt-mediated radical (co)polymerization of vinyl chloride and vinyl acetate*. *Polym. Chem.* 2012, 3, 2880–2891.
- (52) Banerjee, S.; Ladmiral, V.; Debuigne, A.; Detrembleur, C.; Poli, R.; Ameduri, B. *Organometallic-Mediated Radical Polymerization of Vinylidene Fluoride*. *Angew. Chem., Int. Ed.* 2018, 57, 2934–2937.
- (53) Kermagoret, A.; Debuigne, A.; Jérôme, C.; Detrembleur, C. *Precision design of ethylene- and polar-monomer-based copolymers by organometallic-mediated radical polymerization*. *Nat. Chem.* 2014, 6, 179–187.
- (54) Demarteau, J.; Kermagoret, A.; Jérôme, C.; Detrembleur, C.; Debuigne, A. *Controlled synthesis of ethylene-vinyl acetate based copolymers by organometallic mediated radical polymerization*. *ACS Symposium Series, 2015; Vol. 1188 (Controlled Radical Polymerization)*, pp 47–61.
- (55) Demarteau, J.; De Winter, J.; Detrembleur, C.; Debuigne, A. *Ethylene/vinyl acetate-based macrocycles via organometallic-mediated radical polymerization and CuAAC “click” reaction*. *Polym. Chem.* 2018, 9, 273–278.
- (56) Frisch, M. J.; Trucks, G. W.; Schlegel, H. B.; Scuseria, G. E.; Robb, M. A.; Cheeseman, J. R.; Scalmani, G.; Barone, V.; Mennucci, B.; Petersson, G. A.; Nakatsuji, H.; Caricato, M.; Li, X.; Hratchian, H. P.; Izmaylov, A. F.; Bloino, J.; Zheng, G.; Sonnenb, D. J. *Gaussian 09, Revision D.01*; Gaussian, Inc.: Wallingford, CT, 2009.
- (57) Reiher, M. *Theoretical Study of the Fe(phen)2(NCS)2 SpinCrossover Complex with Reparametrized Density Functionals*. *Inorg. Chem.* 2002, 41, 6928–6935.
- (58) Ehlers, A. W.; Böhme, M.; Dapprich, S.; Gobbi, A.; Höllwarth, A.; Jonas, V.; Köhler, K. F.; Stegmann, R.; Veldkamp, A.; Frenking, G. *A set of f-polarization functions for pseudo-potential basis sets of the transition metals Sc-Cu, Y-Ag and La-Au*. *Chem. Phys. Lett.* 1993, 208, 111–114.
- (59) Grimme, S.; Antony, J.; Ehrlich, S.; Krieg, H. *A consistent and accurate ab initio parametrization of density functional dispersion correction (DFT-D) for the 94 elements H-Pu*. *J. Chem. Phys.* 2010, 132, 154104.
- (60) Bryantsev, V. S.; Diallo, M. S.; Goddard III, W. A., III *Calculation of Solvation Free Energies of Charged Solutes Using Mixed Cluster/Continuum Models*. *J. Phys. Chem. B* 2008, 112, 9709–9719.
- (61) Fineman, M.; Ross, S. D. *Linear method for determining monomer reactivity ratios in copolymerization*. *J. Polym. Sci.* 1950, 5, 259–262.
- (62) Kelen, T.; Tüdös, F. *Analysis of the Linear Methods for Determining Copolymerization Reactivity Ratios. I. A New Improved Linear Graphic Method*. *J. Macromol. Sci., Part A: Pure Appl. Chem.* 1975, 9, 1–27.
- (63) Wamsley, A.; Jasti, B.; Phiasivongsa, P.; Li, X. *Synthesis of random terpolymers and determination of reactivity ratios of N-carboxyanhydrides of leucine,  $\beta$ -benzyl aspartate, and valine*. *J. Polym. Sci., Part A: Polym. Chem.* 2004, 42, 317–325.
- (64) Ting, J. M.; Navale, T. S.; Bates, F. S.; Reineke, T. M. *Precise compositional control and systematic preparation of multimonomeric statistical copolymers*. *ACS Macro Lett.* 2013, 2, 770–774.
- (65) Skeist, I. *Copolymerization: the Composition Distribution Curve*. *J. Appl. Chem. Sci.* 1946, 68, 1781–1784.
- (66) García-Álvarez, J.; Díez, J.; Vidal, C. *Pd(ii)-catalyzed cycloisomerisation of  $\gamma$ -alkynoic acids and one-pot tandem cycloisomerisation/CuAAC reactions in water*. *Green Chem.* 2012, 14, 3190–3196.

- (67) Saavedra, B.; Pérez, J. M.; Rodríguez-Álvarez, M. J.; García-Álvarez, J.; Ramon, D. J. Impregnated palladium on magnetite as a water compatible catalyst for the cycloisomerization of alkynoic acid derivatives. *Green Chem.* 2018, 20, 2151–2157.
- (68) Rodríguez-Álvarez, M. J.; Vidal, C.; Díez, J.; García-Álvarez, J. Introducing Deep Eutectic Solvents as Biorenewable Media for Au(I) Catalysed Cycloisomerisation of  $\gamma$ -Alkynoic Acids: An Unprecedented Catalytic System. *Chem. Commun.* 2014, 50, 12927–12929.
- (69) Ramsay, W. J.; Bell, N. A. W.; Qing, Y.; Bayley, H. Single-Molecule Observation of the Intermediates in a Catalytic Cycle. *J. Am. Chem. Soc.* 2018, 140, 17538–17546.
- (70) Fernandes, T. A.; Galvão, A. M.; do Rego, A. M. B.; Carvalho, M. F. N. N. Cu(I) Camphor Coordination Polymers: Synthesis and Study of the Catalytic Activity for Cyclization of 4-Pentyn-1-ol. *J. Polym. Sci., Part A: Polym. Chem.* 2014, 52, 3316–3323.
- (71) Naidu, S.; Rajasekhara Reddy, S. A Green and Recyclable Copper and Ionic Liquid Catalytic System for the Construction of Poly-heterocyclic Compounds via One-pot Tandem Coupling Reaction. *ChemistrySelect* 2017, 2, 1196–1201.
- (72) Leconte, N.; du Moulinet d'Hardemare, A.; Philouze, C.; Thomas, F. A Highly Active Diradical Cobalt(III) Catalyst for the Cycloisomerization of Alkynoic Acids. *Chem. Commun.* 2018, 54, 8241–8244.
- (73) Maria, S.; Kaneyoshi, H.; Matyjaszewski, K.; Poli, R. Effect of Electron Donors on the Radical Polymerization of Vinyl Acetate Mediated by  $[Co(acac)_2]$ : Degenerative Transfer versus Reversible Homolytic Cleavage of an Organocobalt(III) Complex. *Chem.–Eur. J.* 2007, 13, 2480–2492.
- (74) Debuigne, A.; Poli, R.; Jérôme, R.; Jérôme, C.; Detrembleur, C. Key role of metal-coordination in cobalt-mediated radical polymerization of vinyl acetate. *ACS Symposium Series*, 2009, Vol. 1024, pp 131–147.
- (75) Debuigne, A.; Caille, J.-R.; Willet, N.; Jérôme, R. Synthesis of poly(vinyl acetate) and poly(vinyl alcohol) containing block copolymers by combination of cobalt-mediated radical polymerization and ATRP. *Macromolecules* 2005, 38, 9488–9496.
- (76) Detrembleur, C.; Stoilova, O.; Bryaskova, R.; Debuigne, A.; Mouithys-Mickalad, A.; Jérôme, R. Preparation of well-defined PVOH/C60 nanohybrids by cobalt-mediated radical polymerization of vinyl acetate. *Macromol. Rapid Commun.* 2006, 27, 498–504.
- (77) Bryaskova, R.; Willet, N.; Debuigne, A.; Jérôme, R.; Detrembleur, C. Synthesis of Poly(vinyl acetate)-*b*-Polystyrene and Poly(vinyl alcohol)-*b*-Polystyrene copolymers by Cobalt-Mediated Radical Polymerization. *J. Polym. Sci., Part A: Polym. Chem.* 2007, 45, 81–89.
- (78) Park, S.-S.; Yoon, H.-S. Acid-Catalyzed Hydrolysis Reaction of Poly(vinyl acetate). *Polymer (Korea)* 2005, 29, 304–307.
- (79) Hassan, C. M.; Peppas, N. A. Structure and Applications of Poly(vinyl alcohol) Hydrogels Produced by Conventional Crosslinking or by Freezing/Thawing Methods. *Biopolymers: PVA Hydrogels, Anionic Polymerisation Nanocomposites; Advances in Polymer Science; Springer*, 2000, Vol. 153, pp 37–65.
- (80) Debuigne, A.; Willet, N.; Jérôme, R.; Detrembleur, C. Amphiphilic poly(vinyl acetate)-*b*-poly(*N*-vinylpyrrolidone) and novel double hydrophilic poly(vinyl alcohol)-*b*-poly(*N*-vinylpyrrolidone) block copolymers prepared by cobalt-mediated radical polymerization. *Macromolecules* 2007, 40, 7111–7118.
- (81) Bernard, J.; Favier, A.; Zhang, L.; Nilasaroya, A.; Davis, T. P.; Barner-Kowollik, C.; Stenzel, M. H. Poly(vinyl ester) Star Polymers via Xanthate-Mediated Living Radical Polymerization: From Poly(vinyl alcohol) to Glycopolymers Stars. *Macromolecules* 2005, 38, 5475–5484.

- (82) *Harrisson, S.; Liu, X.; Ollagnier, J.-N.; Coutelier, O.; Marty, J.D.; Destarac, M. RAFT Polymerization of Vinyl Esters: Synthesis and Applications. Polymers 2014, 6, 1437–1488.*
- (83) *Arai, K.; Okuzono, M.; Shikata, T. Reason for the High Solubility of Chemically Modified Poly(vinyl alcohol)s in Aqueous Solution. Macromolecules 2015, 48, 1573–1578.*